



Numerical modeling of multiphase flow in porous media considering micro- and nanoscale effects: A comprehensive review

Jianchao Cai^{a,*}, Xiangjie Qin^a, Xuanzhe Xia^a, Xinghe Jiao^a, Hao Chen^b, Han Wang^a, Yuxuan Xia^a

^a State Key Laboratory of Petroleum Resources and Engineering, China University of Petroleum, Beijing, 102249, PR China

^b School of Geophysics and Geomatics, China University of Geosciences, Wuhan, 430074, PR China

ARTICLE INFO

Keywords:

Multiphase flow
Micro- and nanoporous media
Molecular dynamics simulation
Pore scale simulation

ABSTRACT

Multiphase flow in porous media involves a variety of natural and industrial processes. However, the microscopic description of multiphase flow is challenging due to fluid-fluid and fluid-solid interactions combined with complex pore topology. Thus, a systematic review of multiphase flow from molecular to pore scale perspectives is necessary. This work summarizes recent progress in numerical modeling of multiphase flow from molecular scale, pore scale, and reservoir scale simulations considering micro- and nanoscale effects. The analysis focuses on immiscible and miscible flow associated with liquid and gas phases, highlighting the micro- and nanoscale effects on the flow characteristics. Molecular simulations capture nanoscale effects such as adsorption, diffusion, and slip behaviors. The variation of wettability, pressure, and fluid saturation leads to film, slug, and droplet flows in nanopores. Pore scale simulations explain complex flow behaviors in microporous and nanoporous media. Capillary number and wettability lead to different invasion morphologies. Adsorption and slip effects are non-negligible for fluid flow in nanoporous media. Furthermore, there are obvious differences in reservoir simulation results with and without considering micro- and nanoscale effects. Generally, this in-depth review is intended to provide a comprehensive description of the multiphase flows through multiscale simulation methods being developed and assist industrial processes.

Nomenclature

Parameters	
A	Pore cross-section area
A_b	Bulk region area
A_w	Confined region area
d	Distance from pore center
h	Rectangular capillary height
K_n	Knudsen number
L	Capillary length
l	Mean free path of free gas molecules
l_s	Slip length
M	Viscosity ratio
P	Pressure
P_c	Capillary pressure of a circular capillary
P_r	Capillary pressure of a rectangular capillary
r	Pore radius
u	Velocity
u_s	Slip velocity
u_w	Near-wall phase fluid velocity

(continued on next column)

(continued)

w	Rectangular capillary width
γ	Interfacial tension
θ	Contact angle
μ	Liquid viscosity
μ_b	Bulk phase fluid viscosity
μ_{eff}	Effective fluid viscosity
μ_w	Near-wall phase fluid viscosity
λ	Pore diameter
Abbreviations	
Ca	Capillary number
DPD	Dissipative particle dynamics
DNS	Direct numerical simulation
EOR	Enhanced oil recovery
HP	Hagen-Poiseuille
LB	Lattice Boltzmann
LBM	Lattice Boltzmann method
LS	Level set
MMP	Minimum miscible pressure
MC	Monte Carlo

(continued on next page)

* Corresponding author.

E-mail address: caijc@cup.edu.cn (J. Cai).

<https://doi.org/10.1016/j.jgsce.2024.205441>

Received 5 June 2024; Received in revised form 21 August 2024; Accepted 7 September 2024

Available online 10 September 2024

2949-9089/© 2024 Elsevier B.V. All rights are reserved, including those for text and data mining, AI training, and similar technologies.

(continued)

MD	Molecular dynamics
PNM	Pore network model
TOC	Total organic carbon
VOF	Volume of fluid

1. Introduction

Multiphase flow is defined as the transport behaviors consisting of gas-liquid-solid in the same space simultaneously, and plays a non-negligible role in many fields of natural science and engineering, such as coal-biomass flow in power plants (Yan et al., 2018), gas-water flow in fuel cells (Kone et al., 2017), gas-liquid flow in bubble column reactors (Fard et al., 2020), gas-liquid-particle flow during drug delivery (Farnoud et al., 2020; Rahimi-Gorji et al., 2022), and oil-gas-water-solid flow in oil/gas reservoirs (Patel et al., 2019; Zhu et al., 2021; Liu et al., 2022b). Due to fluid-fluid and fluid-solid interactions, the multiphase flow process is complex compared to the well-understood single-phase fluid flows (Wang et al., 2021a). Multiphase flow behaviors in complex porous media are uncertain due to the complicated pore throat structures and phase distributions (Bakhshian et al., 2019). Especially in the field of hydrocarbon extraction, the porous media is composed of a variety of minerals and has multiscale characteristics from nm to m. This results in the coexistence of different multiphase fluids (oil-water, oil-gas, gas-water, water-solid, oil-CO₂, oil-CO₂-water, etc.), leading to complex multiphase flow behaviors in porous media (Foroozesh and Kumar, 2020; Zhang et al., 2024). Clarifying the multiphase flow behaviors in complex porous media is extremely important, not only for hydrocarbon extraction but also for theoretical and engineering applications.

The research methods for studying multiphase flow in porous media include experiment, theory, and numerical simulation. Core-scale displacement experiment is a commonly used method to study multiphase flow, and couples with online nuclear magnetic resonance to observe the multiphase fluid distribution simultaneously (Baban et al., 2023; Tang et al., 2023). Although the core-scale experiment is an effective method to obtain macroscopic application parameters, it cannot accurately characterize the interface dynamics in realistic pore spaces and then explore the microscopic mechanism affecting the macroscopic flow characteristics. Fortunately, the pore scale microfluidic experimental methods can intuitively visualize the interface dynamics and multiphase distributions, and then the microscopic migration mechanisms can be clarified (Gogoi and Gogoi, 2019). However, microfluidic chips have certain limitations in terms of pore size and experimental conditions, such as nanoscale microfluidic chips and high temperature/pressure experimental conditions that are difficult to achieve. Meanwhile, the microfluidic chip is generally a two-dimensional (2D) structure and cannot accurately represent the spatial migration mechanisms of multiphase fluids in a three-dimensional (3D) structure. Moreover, experiments associated with nanoscale porous media are highly expensive. At present, scholars have employed theoretical methods to characterize the layered flow of oil-water and gas-water (Wang et al., 2019a; Tian et al., 2022a), as well as the spontaneous and forced imbibition behaviors in nanoscale pores (Li et al., 2022; Tian et al., 2022). Based on the capillary tube bundles, the theoretical equation of confined liquid flow in single nanopores is extended to porous media (Cai et al., 2014). However, realistic porous media exhibit complex pore structures and heterogeneous wettability; therefore, the ideal theoretical approach lacks accuracy and is no longer applicable.

With the development of computer technology, the numerical simulation method is popular with the advantages of safety, high efficiency, accuracy, and low consumption in simulating multiphase flows. According to the modeling scale, numerical simulation can be divided into molecule scale, pore scale, and macroscale methods. The

macroscale numerical method simulates the multiphase flow by solving the continuity equation and then obtains the macroscopic parameters. Similar to the core-scale experiment, the macroscale numerical simulation ignores the complex pore structure of porous media and cannot accurately clarify the multiphase fluid distribution and migration mechanisms. Alternatively, molecule scale and pore scale numerical methods can effectively capture the evolution of multiphase interfaces in various pore structures and are ideal methods to intuitively and accurately explain the microscopic multiphase flow mechanisms (Golparvar et al., 2018; Chen et al., 2022). Among them, the molecular dynamics (MD) method can accurately capture the interaction forces between fluid-fluid and fluid-solid molecules, and truly simulate the dynamic and static physical and chemical behaviors of fluids in micro- and nanoscale pores (Cai et al., 2024a; Wu et al., 2024). For example, by simulating the static distribution behavior of multiphase fluids on different mineral surfaces and in different mineral pores, the wettability characteristics and adsorption effects caused by fluid-solid forces can be calculated (Chen et al., 2020; Sun and Bourg, 2020; Yang et al., 2020). By simulating the multiphase flow behavior in nanoconfined spaces, the fluid-fluid and fluid-solid interaction parameters with different mineral compositions can be calculated (Zhang et al., 2021b). Due to computational limitations, current physics models for MD simulation are typically restricted to single nanopores or simplified pore-throat structures. Moreover, the pore scale simulation can extend the multiphase flow in a single nanopore to a porous media with complex structures. The influence mechanisms of pore structure properties, heterogeneous wettability, and micro- and nanoscale effects on the flow behaviors of multiphase fluid in porous media can be further explored. The pore scale simulation is generally used to simulate the multiphase flow behavior in complex pore structures under the action of capillary force and viscous force (Zhao et al., 2023). However, it is impossible to calculate the microscopic phenomena caused by intermolecular forces, such as the different slip lengths and wettability characteristics of different mineral surfaces, and these parameters are usually set manually. In nanoscale porous media, the parameters caused by the intermolecular interaction forces can be calculated by MD simulation, and the pore scale simulation of multiphase flow can be carried out to analyze the flow mechanisms.

Currently, extensive research has been conducted on the numerical simulations of multiphase flow processes. These studies include the theoretical methods and MD simulations for multiphase flow within single nanopores (Fig. 1(a) and (b)), as well as pore scale modeling for the complex flow processes within porous media (Fig. 1(c)). In addition, reservoir simulations considering micro- and nanoscale effects have been developed (Fig. 1(d)), achieving satisfactory progress. Therefore, this work systematically reviews multiphase flow from the molecular scale, pore scale to the reservoir scale according to the scale upgrading scheme (Fig. 2). Firstly, the fluid-fluid and fluid-solid interaction mechanisms involved in the multiphase flow process are theoretically analyzed in Section 2. Then, MD simulations are introduced in Section 3 to explain the effects of these microscopic mechanisms on multiphase flows within single nanopores. To improve the modeling scale for analyzing multiphase fluid flow in complex porous media, Section 4 introduces pore scale simulation methods that consider micro- and nanoscale effects. Finally, the impact of micro- and nanoscale effects on reservoir simulation results is discussed in Section 5 to illustrate the practical significance of this review.

2. Micro- and nanoscale effects in multiphase flow

Single-phase and multiphase flow processes are affected by micro- and nanoscale effects. Slip means that the fluid has a certain tangential velocity at the pore surface, which affects liquid and gas flow in the nanochannel. Contact angle and interfacial tension play a significant role in multiphase fluid transport. Fluid-fluid and fluid-solid interactions are manifested as capillary and slip effects.

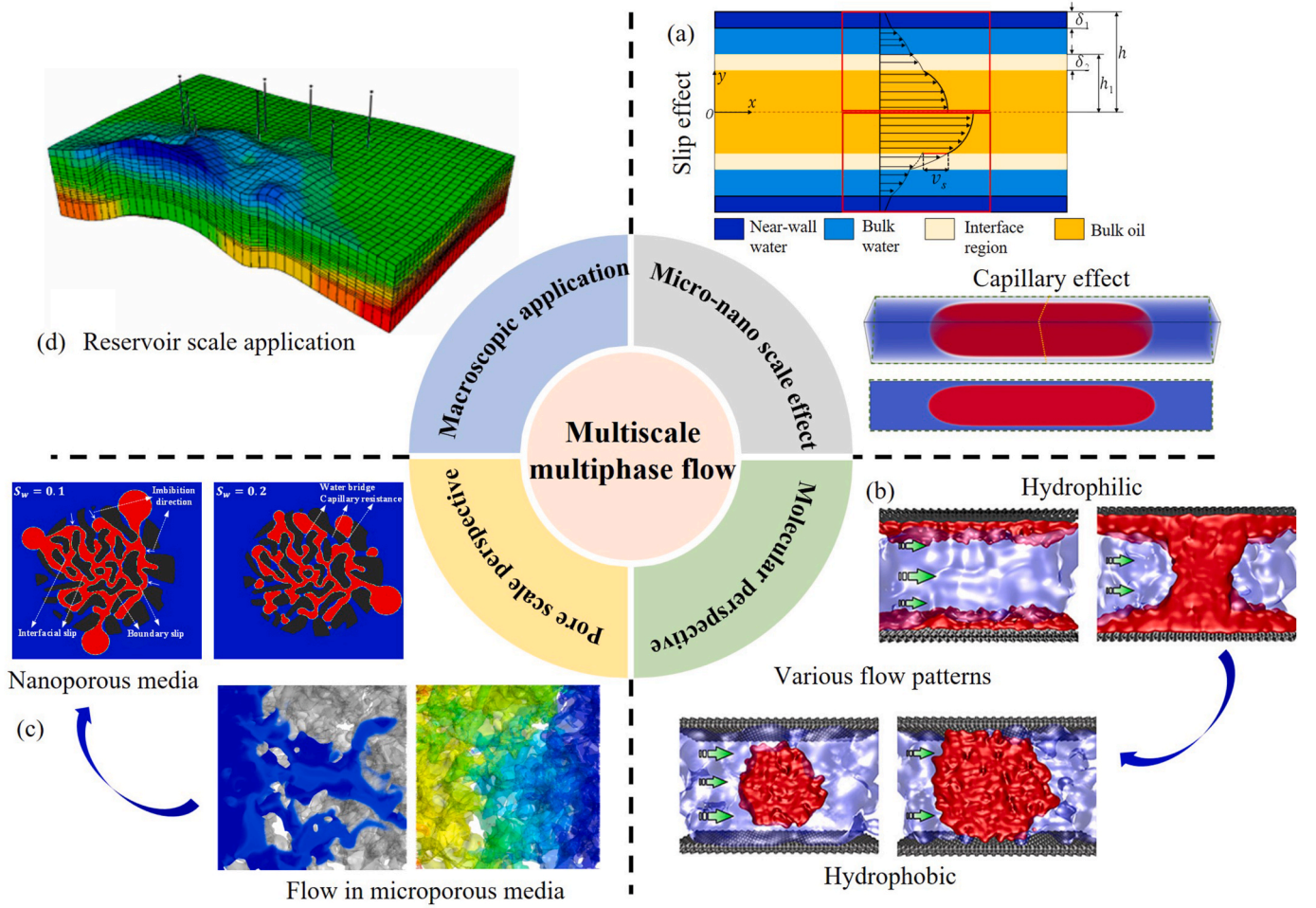


Fig. 1. Description of (a) multiphase flow mechanism considering micro- and nanoscale effects, and the multiphase flow process at (b) molecular scale (Xu et al., 2020), (c) pore scale (Cai et al., 2024), and (d) reservoir scale (Hovorka et al., 2009).

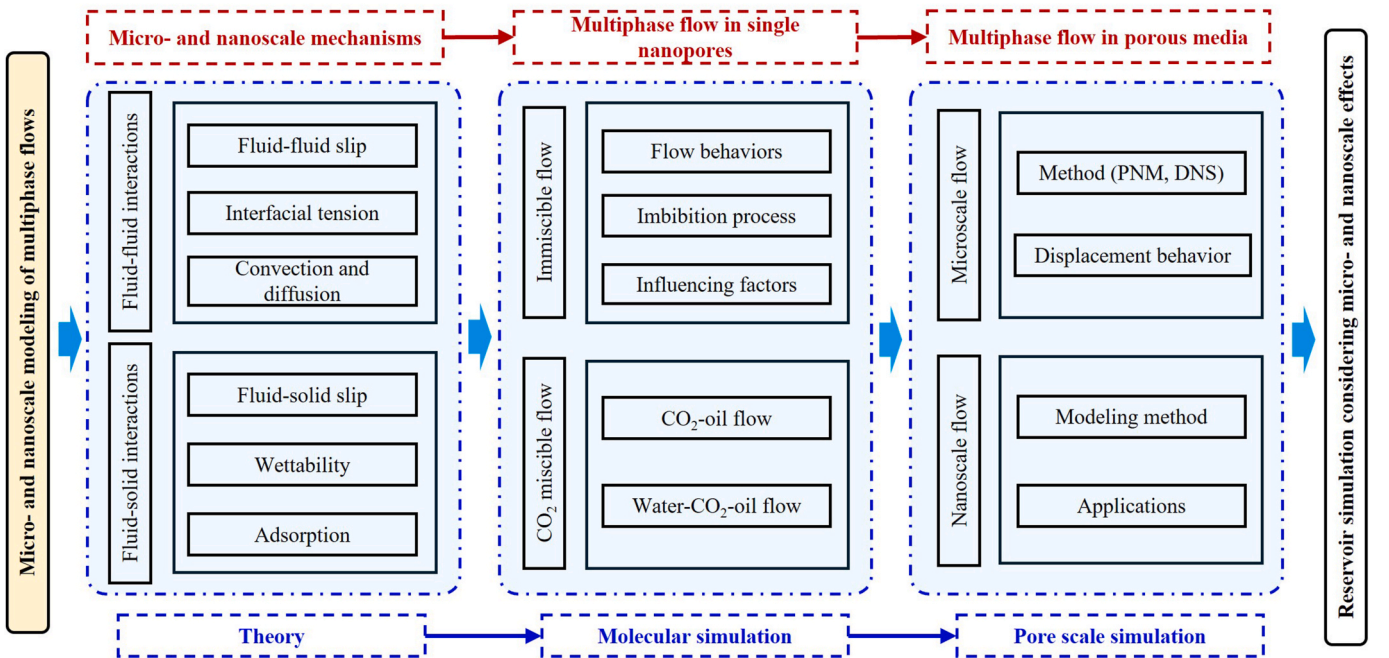


Fig. 2. Comprehensive analysis flowchart.

2.1. Liquid transport

The flow velocity profile of liquid in conventional scale pores is a typical parabolic shape, which can be calculated by the Hagen-Poiseuille (HP) equation:

$$u = \frac{\Delta P(r^2 - d^2)}{4\mu L} \quad (1)$$

where u is velocity, r is pore radius, d is distance from pore center, μ is liquid viscosity, $\Delta P/L$ is pressure gradient. However, in the nanoscale pores, the liquid-solid interaction force cannot be ignored, resulting in a liquid flow velocity greater than 0 on the mineral surface (Fig. 3 (a)), which is defined as the slip velocity u_s . The slip velocity can be calculated by the slip length l_s and velocity gradient:

$$u_s = -l_s \left. \frac{\partial u_w}{\partial r} \right|_{d=r} \quad (2)$$

where u_w is the velocity of the near-wall phase fluid.

The slip length is typically within the nanoscale range and comparable to the dimensions of nanopores (Thomas and McGaughey, 2008; Secchi et al., 2016), thus emphasizing the importance of slip in affecting flow capacity (Wu et al., 2017). Compared with the volume flux predicted by the classical no-slip HP equation, the flow capacity considering

the slip effect is increased by $10^0 \sim 10^7$ times (Wu et al., 2017). In conventional scale pores, nanoscale slip lengths also exist on the mineral surface, but their impact is negligible due to the large pore size. Therefore, the consideration of slip effects is unnecessary in conventional theoretical and simulation methods.

In addition to the slip velocity caused by the liquid-solid interaction force, it also causes the heterogeneous viscosity of the liquid (Qin et al., 2024a), that is, the viscosity of the near-wall phase fluid (μ_w) is different from that of the bulk phase fluid (μ_b) due to the influence of the solid molecular interaction forces on the fluid molecules in the near-wall region. The heterogeneous viscosity can be expressed by the effective viscosity (μ_{eff}) calculated by area weighting (Thomas and McGaughey, 2008):

$$\mu_{eff} = \mu_w \frac{A_w}{A} + \mu_b \frac{A_b}{A} \quad (3)$$

where A_w , A_b and A are the area of the confined region, bulk region, and pore cross-section. According to molecular simulation, there are about 2 layers of molecules near the wall affected by the molecular interaction force of the solid, and the near-wall thickness of the oil and water phase is about 1 nm and 0.7 nm (Zhang et al., 2017). When the liquid-solid adhesion force is large, the effective slip length will be negative, that is, the velocity of the near-wall liquid is about 0. Under the influence of

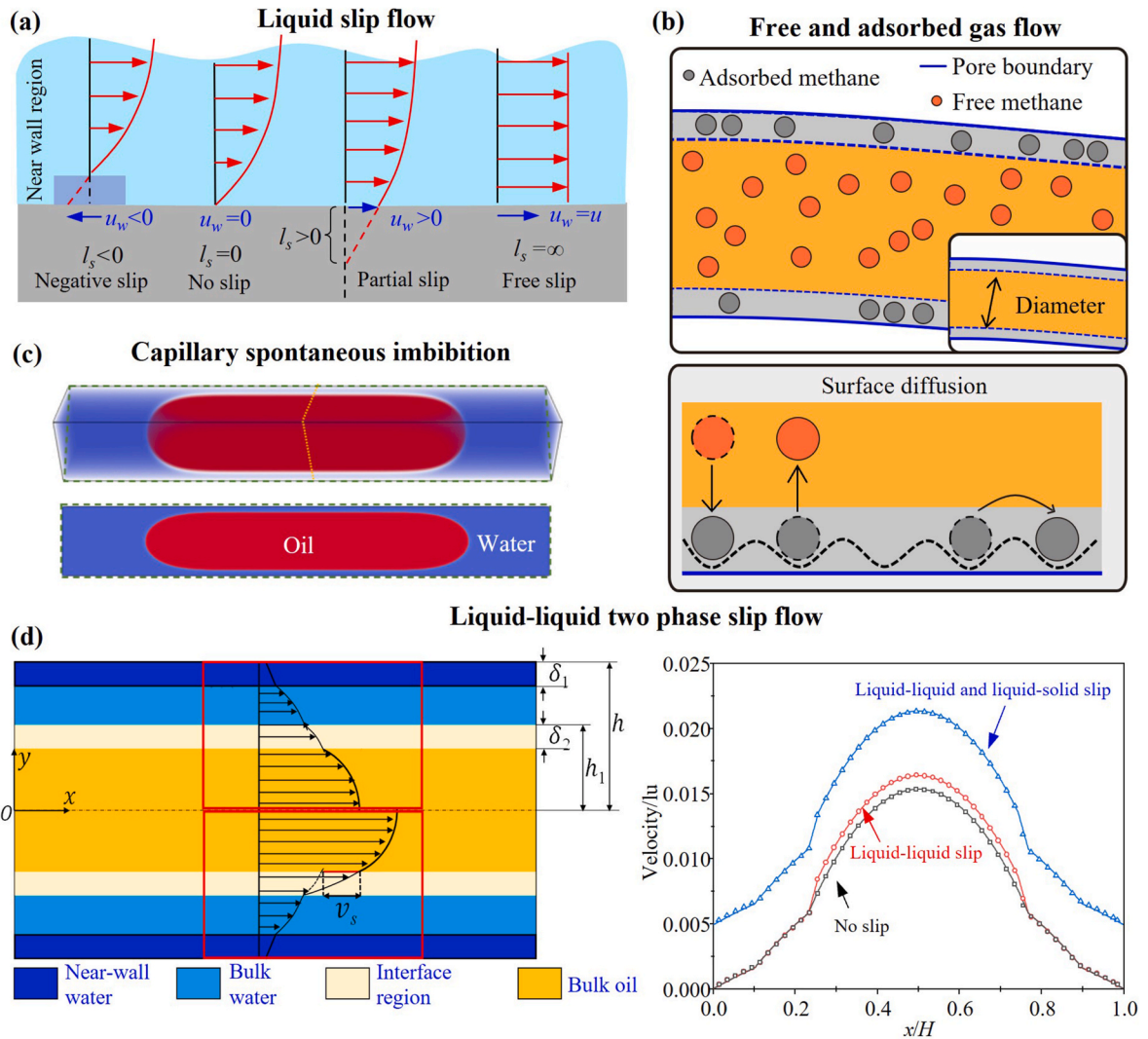


Fig. 3. Micro- and nanoscale effects in fluid flow. (a) Liquid slip flow regimes (Qin et al., 2024a). (b) Free and adsorbed gas flow. (c) Spontaneous imbibition in rectangular capillaries (Liu et al., 2022b). (d) Liquid-liquid slip flow in nanoscale pores (Wang et al., 2022).

different liquid-solid interaction forces, the near-wall viscosity is about 0.1–10 times that of the bulk viscosity. The flow capacity is increased by 0.1–10 times compared with the volume flow predicted by the classical no-slip HP equation.

2.2. Gas transport

For viscous flow, the gas molecules mostly collide with other molecules during their movements, and the collisions with the pore surface can be ignored. The situation is quite different from the viscous flow when the gas molecules transport through nanoscale pores. On one hand, the mean free path of free gas molecules (l) is approaching or larger than the characteristic length of the pore (usually takes the pore diameter (λ)), therefore, the interactions between the gas molecules and the pore surface becoming more frequent and cannot be ignored. On the other hand, the strong attraction between the pore surface and gas molecules results in parts of gas molecules existing in the adsorbed state, whose transport characteristics are also different from that of the free gas (i.e., bulk gas). Therefore, the transport mechanisms of free gas and adsorbed gas should be analyzed, respectively (Fig. 3 (b)).

Knudsen number (K_n) is usually introduced to judge the flow regimes of free gas, which is defined as:

$$K_n = \frac{l}{\lambda} \quad (4)$$

The flow regimes of free gas are divided into: (1) viscous flow/continuum flow regime ($K_n < 10^{-3}$), gas molecules densely filled in microscale pores. Euler equation is accurate for the gas transport prediction of viscous flow. For isodiametric pores with circular cross-sections, the gas flow rate can be calculated by the Hagen-Poiseuille equation. (2) Slip flow regime ($10^{-3} \leq K_n < 10^{-1}$), the gas velocity near the pore surface is not zero anymore with the decrease of pore size, still intermolecular collision dominated. In this case, the Navier-Stokes equations coupling with different slip boundary conditions (Struchtrup, 2005; Javadpour et al., 2021) are usually used to depict the gas flow. Except for the convection effects of viscous flow and slip flow, Fick's diffusion also occurs when $K_n < 0.1$. However, the gas permeability of Fick's diffusion is much smaller than that of viscous flow and slip flow. (3) Transition diffusion regime ($10^{-1} \leq K_n < 10^1$), the intermolecular collision, and the gas molecule-pore surface collision are of equal importance for gas flow. (4) Free molecule flow regime/Knudsen diffusion regime ($K_n \geq 10^1$), the gas molecules are rarefied in small nanoscale pores, and the collisions are gas molecule-pore surface dominated (Gilron and Soffer, 2002; Roy et al., 2003; Mo et al., 2022).

Adsorbed gas molecules are not static but mobile, and surface diffusion is an important transport mechanism, which is crucial for nanoscale pores with strong adsorption capacity, such as shale and coal (Tian et al., 2022b; Wang et al., 2024a). There are primarily two approaches to studying the mechanism of surface diffusion. One is Fick's law, which relies on the concentration gradient of adsorbed gas as the driving force (Xiong et al., 2012; Wu et al., 2016a; Cai et al., 2019); and the other is Maxwell-Stefan theory-based, which is driven by the chemical potential gradient (Wu et al., 2015; He et al., 2017; Zhang et al., 2019a).

2.3. Multiphase transport

Multiphase flow in microporous and nanoporous media is a complex process. In addition to the flow mechanisms involved in single-phase gas and liquid flow, complex interfacial interactions should also be considered, including capillary effects, two-phase interactions, and three-phase interactions.

2.3.1. Capillary effect

The capillary force is the pressure difference between the immiscible wetting and the non-wetting fluids on both sides of the interface. The

capillary force is equal to the component force of the interfacial tension force along the flow direction. For circular capillaries, capillary pressure (P_c) is calculated based on Laplace's equation:

$$P_c = \frac{2\gamma}{r} \cos \theta \quad (5)$$

where γ is the interfacial tension, θ is the contact angle.

The magnitude of the capillary force is closely related to the interaction between the fluid and the solid surface (i.e. contact angle) (Liu et al., 2022b), the fluid-fluid interaction (i.e. interfacial tension) (Feng et al., 2022), and the capillary radius. The increasing contact angle reduces the fluid-solid interaction. While the contact angle is not a specific value in the actual flow process (Li et al., 2023). Receding and advancing contact angles are formed as the liquid flows on the rough surface (contact angle hysteresis). Advancing contact angle reflects the fluid-solid cohesion, receding contact angle reflects the fluid-solid adhesion. An increase in flow velocity results in an increase in the advancing contact angle and a decrease in the receding contact angle. Moreover, the interfacial tension is proportional to the capillary pressure and is constant in immiscible flows. However, for the CO₂ miscible flow, convection and diffusion are the main fluid transport mechanisms. The CO₂ dissolved in the liquid phase reduces the fluid viscosity and interfacial tension, enhancing the displacement efficiency (Wang et al., 2023b).

Capillary shape is a key factor in controlling capillary force. The perimeter of the liquid-solid interface corresponding to the complex capillary shape is large, resulting in higher capillary pressure. The capillary pressure for a rectangular capillary (height, h , and width, w) is given by Dong Sung et al. (2002):

$$P_c = 2\gamma \left(\frac{1}{h} + \frac{1}{w} \right) \cos \theta \quad (6)$$

The wetting fluid invades the non-wetting system by capillary force under hydrophilic conditions, (i.e. spontaneous imbibition). The interface curvature of the two phases is negative during imbibition, and corner flow may occur in rectangular capillary due to the large capillary force in the corners (Fig. 3 (c)). The interface curvature is positive under hydrophobic conditions; the wetting fluid relies on external forces to displace wetting fluids.

The capillary force is not negligible in micro- and nanoscale multiphase flows. During drainage, the displacement is significantly affected by narrow throat structures that correspond to large capillary resistance. This causes the Haynes jumps and the entrainment of the non-wetting fluid within the wetting fluid. In contrast, the imbibition process is controlled by pore-throat structures that correspond to positive capillary forces, and the displacement mechanism is complicated due to the corner film flow, piston-like displacement, and snap-off events.

2.3.2. Slip effect

The fluid-fluid and fluid-solid interfaces are assumed to be no slip in homogeneous immiscible two-phase flow. However, the velocity of the two phases is quite different due to the liquid-liquid slip and liquid-solid slip in nanoconfined multiphase flows (Vega-Sánchez et al., 2022; Wang et al., 2023a), as displayed in Fig. 3 (d). Unlike the macroscale multiphase flow, the nanoconfined multiphase flow in nanoporous media involves a variety of flow regimes. It includes adsorption, diffusion, fluid-solid slip, and the fluid-fluid slip.

Wetting and non-wetting fluids exhibit different flow behaviors on pore surfaces. The hydrophilic pore surface restricts the flow of wetting fluids, while the flow of non-wetting fluid is enhanced due to weak fluid-solid interaction (Qin et al., 2024b). Not only solid-liquid slip between fluid-solid interface but also liquid-liquid slip caused by heterogeneous viscosity occurs at the near-wall region. This results in stratified velocity distribution in the capillary. In addition, the liquid-liquid slip caused by heterogeneous viscosity occurs at the interface region of two phases,

Table 1

Various flow behaviors in nanopores.

Reference	Method	Flow types	Analysis factors	Conclusions
Takaba et al. (2007)	Nonequilibrium MD technique	Film flow	Poiseuille flow of molecular thin fluid	Strong membrane-wall interaction corresponds to small film flow velocity, which has a significant effect on density distribution.
Sofos et al. (2010)	Nonequilibrium MD technique	Film flow	The influence of wall roughness on film flow	The shear viscosity of a rough wall is higher than that of the smooth wall, and the diffusion coefficient is smaller near a rough wall.
Kasiteropoulou et al. (2013)	Dissipative particle dynamics	Film flow	Film flow on the wall with periodic groove	Wall roughness diminishes the sliding velocity of the fluid on rough walls.
Yong and Zhou (2022)	Full-atoms MD simulations	Droplet flow	Sliding process of water droplets on rough pore surfaces in the kerogen system	Sliding velocity is related to pressure gradient and surface roughness, and forward contact angle is almost equal to backward contact angle.
Liu et al. (2018)	Equilibrium and nonequilibrium MD simulations	Slug flow	Methane-water flow in hydrophilic nanopores	Flow morphology can be manifested as water film, water bridge, and water column under different pressures, and the flow patterns also depend on wettability.
Xu et al. (2020)	External field non-equilibrium MD	Slug flow	Effect of wettability on gas-water flow in nanopores	For the hydrophilic pore surface, water molecules concentrate in the pore center, forming a water bridge and gas slug.
Xiong et al. (2020)	MD simulations	Slug flow	Methane-water flow in illite nanopores	Positive potassium layer and negative hydroxyl group induced a local electric field, which is conducive to the formation of a water bridge.

resulting a unique velocity profile. Because of these phenomena, there is a difference between the holdups and cuts of the phases compared to no slip flows, and the fluid viscosity varies in different stratified regions (Fig. 3 (d)). In a water-wet nanoscale capillary, the flow regions are divided into adsorbed water, bulk water, water-oil interface layer, and bulk oil (Zhan et al., 2020b).

3. Molecular simulations for nanoscale multiphase flow

Molecular simulation generally refers to the simulation of the structure and behavior of atoms and molecules. Starting from the basic principles of statistical mechanics, it replaces experimental measurements with calculated data and obtains relevant physical and chemical information. The commonly used methods of molecular simulation include MD and Monte Carlo. MD method is based on classical mechanics, quantum mechanics, and statistical mechanics, which aims to research a multi-body system composed of atoms and molecules. It is assumed that each nucleus moves under the action of the empirical potential field generated by all other nuclei and electrons. The nucleus moves according to Newton's law of motion. Monte Carlo method is a statistical sample method that uses random numbers to solve numerical problems. MD simulations provide the ability to investigate multiphase flow mechanisms in nanopores. However, MD simulations are usually limited to single nanopores due to expensive computational resources.

3.1. Immiscible multiphase flow

In immiscible multiphase flow systems, there are distinct interfaces between fluids. Fluid flow and interfacial behavior in nanoconfined pores are affected by wettability, pore topology, and phase distribution. MD simulations can provide detailed information on the viscosity and density distribution within nanoconfined pores, allowing for a better understanding of flow characteristics.

3.1.1. Nanoscale flow behaviors

The thin film flow is complicated due to its free surface. MD simulation method is used to simulate the Couette and Poiseuille flow of molecular film-like fluid, and the velocity distribution of the confined film is distorted (Bitsanis et al., 1987, 1988). This phenomenon is caused by the local film density changes with the film thickness, and the film thickness is only several times the diameter of the fluid molecule. As displayed in Table 1, MD simulations have been applied to explore the film flow characteristics in different types of nanochannels. Due to the strong affinity between the solid surface and the fluid, the film flow velocity is limited. Besides, the wall roughness also has an important

effect on the film flow in nanochannels. For fluid film confined in a nanochannel, the roughness of the wall surface could influence the shear viscosity. Slug and droplet flow are potential flow patterns in micro- and nanoscale immiscible two-phase flows. Slug flow consists of a sequence of bubbles or slugs having the consistent width as the tube. Each bubble or slug is surrounded by a thin layer of the carrying phase and is separated by slugs (Yao et al., 2015; Etmnan et al., 2023). In capillaries less than 2 mm in diameter, due to strong interface effects and viscous forces, slug and droplet flow is the dominant flow state (Kreutzer et al., 2005; Ufer et al., 2011). Especially at the nanoscale, the flow mechanism is more complex due to the slip effect. The application of MD simulations in slug and droplet flow is investigated (Table 1). The sliding velocity of water droplets on rough kerogen pore surfaces is related to the pressure gradient and surface roughness, and the droplet is barely deformed. For slug flow, wettable fluid molecules form a liquid bridge to separate non-wettable fluid to form slug flow patterns. Actually, the flow patterns in nanopores are affected by wettability, displacement pressure, and fluid saturation. At low wetting fluid saturation, wetting fluids tend to film flow, and as the saturation increases, water bridges are formed, and non-wetting fluids form slugs (Fig. 4 (a)). These complex flow morphologies lead to heterogeneous density distribution in nanopores (Fig. 4 (b)).

For multiphase flow in nanoporous media, the flow mechanism is complex due to the diverse pore shapes and sizes. In fact, MD simulation does not directly obtain the flow properties in porous media subject to computational limitations. Therefore, MD simulation is usually adopted to explore the flow characteristics in different pore types in order to indirectly describe the flow behavior within nanoporous media. Currently, a large number of studies on nanoscale multiphase flow within intricate porous media primarily focus on kerogen, a solid sedimentary organic material that does not dissolve in ordinary organic solvents (Pawar et al., 2017; Zhang et al., 2022a). The kerogen contains a large number of nanoscale pores, with the diameter generally being less than 2 nm (Chalmers et al., 2012). As a result, the flow behavior of fluids in the real kerogen is complex and the transport mechanism in realistic kerogen nanopores is crucial to shale oil and gas production. However, due to differences in biological precursors and maturity, different types of kerogen have different structures (Vandenbroucke and Largeau, 2007), leading to complex pore systems. Based on experimental analysis data, Ungerer et al. (2015) created a 3D model of kerogen for a variety of oil shale types and maturity stages utilizing MD simulations. These models have been extensively employed to analyze the static and dynamic properties of oil and gas within the kerogen matrix. In addition, the presence of water not only competes with the fluid for adsorption sites and interferes with the interactions between

kerogen and the fluid, but also blocks the flow channels (Sui et al., 2020). Gong et al. (2020) developed moist kerogen II-D models and discovered that the presence of water significantly diminishes the volume of accessible pores, consequently resulting in a reduced capacity for methane adsorption. The diffusion capacity of methane will also decrease with the increase of water content. Sang et al. (2022b) conducted simulations to investigate the behavior of methane and water flow within kerogen slits, analyzing how factors such as water saturation, the width of the slits, temperature, and pressure influence the distribution and velocities of the fluids. For hydrophobic kerogen surface, water tends to form water clusters in the gas phase under low water saturation conditions, whereas at high water saturation, water tends to form a water layer in the middle of the pores. The presence of water slightly increases the gas velocity when the water saturation is less than 0.5. When the size of slit is reduced to 2 nm, it becomes challenging to establish a continuous phase of either gas or water. Wu et al. (2023) observed that the adsorption of methane facilitates the merging of water clusters and prevents their lateral expansion along the wall surfaces at high water concentrations.

In addition, particle-based dissipative particle dynamics (DPD), similar to MD simulation, have been applied to simulate multiphase flow in porous media. This is a mesoscale simulation method, where a particle represents a group of molecules and atoms. Therefore, it can perform simulations on larger length and time scales compared to MD simulations (usually 10 nm–1000 nm and 1 ns–10 ms) (Ahmadi et al., 2022). Liu et al. (2007) verified the DPD simulations for multiphase flow in microchannels and complex networks. They concluded that the multiphase flow process is complex in porous media due to the influence of viscosity, capillary force, gravity, and channel structure. In recent years, DPD has been widely used in colloids and interface phenomena related to nanoparticles, surfactants, phase separations, etc. (Santo and Neimark, 2021).

3.1.2. Imbibition process in nanopores

The imbibition process of wetting fluid in nanopores is an important mechanism for enhanced hydrocarbon recovery. The interactions of microscopic forces in nanopores are complex. Oyarzua et al. (2015) classified imbibition into three flow types through MD simulations (Fig. 5 (a)). In the initial regime, capillary force is only balanced by the inertial force, and the formation of meniscus significantly affects the imbibition rate. The impact of inertial and viscous forces is significant in

the transitional regime. Subsequently, a flow regime is formed in which viscous forces dominate the capillary force balance. In addition, the interaction between porous surface and fluid varies with different pore types, which affects the imbibition mechanism. Yang et al. (2017) conducted simulations to study the imbibition process of octane and water molecules within graphite and quartz slits, with varying widths of 1, 1.5, and 2 nm. In quartz slits, the oil and water imbibition rate from MD is quite close to the result from the Handy model. However, in the graphene slits, the imbibition rate of oil and water obtained by MD is significantly higher than the predicted value of the Handy model. This behavior is mainly attributed to the enhanced intermolecular interaction of octane and graphite on the nanopore wall. It is noticed that the existence state of polar molecules in the nanopores also affects the mechanism of imbibition (Fig. 5 (b)). The adsorption energy and the orientation of the molecules are critical factors in defining the state of existence for polar molecules. (Wang et al., 2021b). At the nanoscale, the transport of n-alkane molecules is mainly affected by molecular structure and molecular motion (Fig. 5 (c)). Slit width, temperature, and n-alkane molecules type affect the flow rate (Sang et al., 2022a). The presence of a high concentration of short-chain alkanes, coupled with high temperatures, promotes the movement of the alkane mixture through the kerogen slits.

3.1.3. Influencing factors of nanoscale multiphase flow

For the fluid-solid interactions, the nanopore surface may behave as hydrophobic and hydrophilic (Mu et al., 2023). There is a difference between the flow behavior in hydrophobic and hydrophilic pore surfaces (Fig. 6 (a)). To quantify the effect of fluid-solid slip on liquid flow, the relationship between the slip distance and the contact angle is obtained based on the MD simulations (Huang et al., 2008). As the contact angle increases, the slip distance increases exponentially, indicating that the effect of solid-liquid slip in the nanopores is significant. However, this phenomenon weakens with increasing pore size. Water in the hydrophilic quartz slit leads to the formation of water films. A water cluster locates at the center of the methane phase in a hydrophobic kerogen slit at low water saturation, but a water layer will form at high water saturation. In both wettability conditions, water occupies the flow space and reduces the flow path of the gas. In addition, the multiphase flow in nanopores depends on irreducible water saturation (Li et al., 2017), solid substrate (Bui et al., 2017), and pressure gradient. Due to pressure gradients and wettability, the flow pattern of water will change between

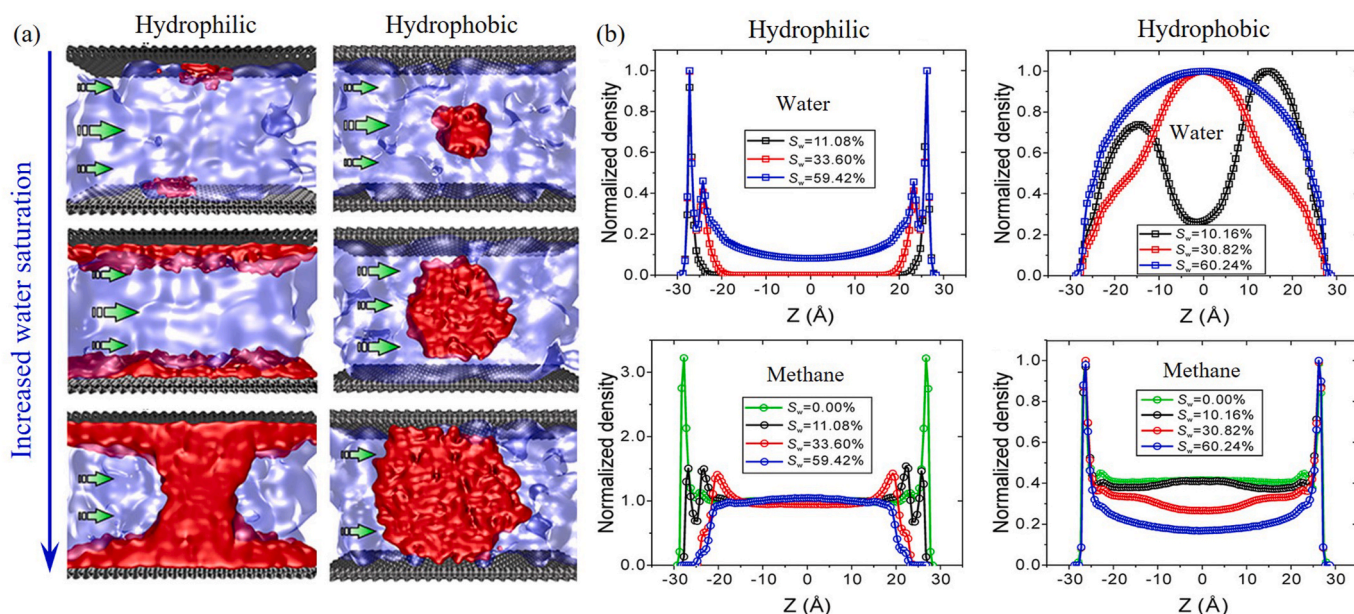


Fig. 4. Water-gas flow in nanopores with different wettability (Xu et al., 2020); (a) Flow patterns; (b) Normalized density distribution of water.

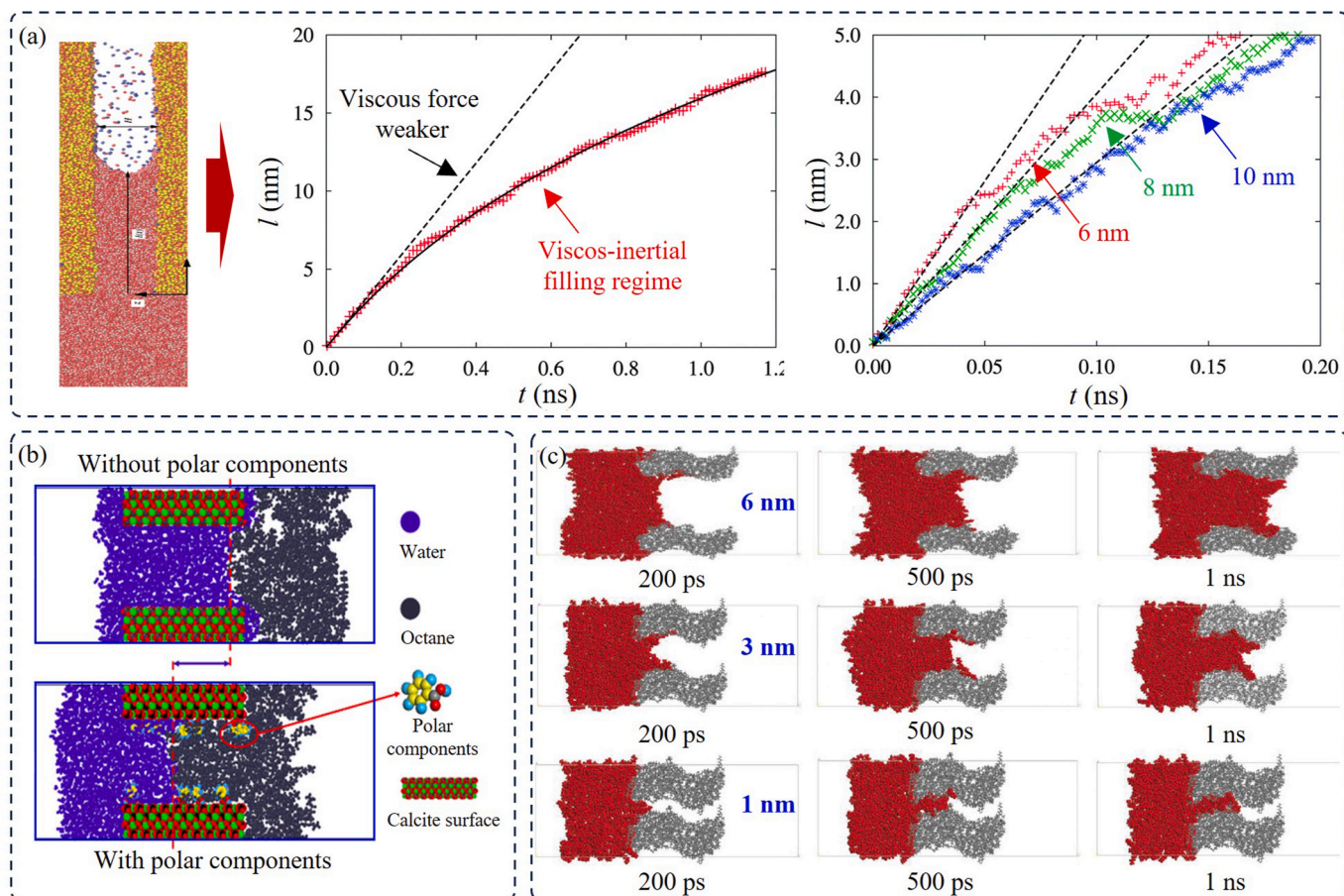


Fig. 5. Characteristics of fluid motion in the imbibition process. (a) Force interactions during imbibition (Oyarzua et al., 2015). (b) Effect of polar molecules on imbibition (Wang et al., 2021b). (c) Imbibition process of n-alkanes in kerogen slits with different widths (Sang et al., 2022a).

the water film, water bridge, and water column (Fig. 6 (b)). This is due to the nonuniform density/viscosity distribution near the surface (Liu et al., 2018).

As for the fluid-fluid interactions, the exchange of momentum between water and methane molecules at the gas-water interface significantly influences the flow characteristics. The occurrence of liquid-liquid slip within nanopores should not be disregarded. For octane

flow in quartz nanopore with the presence of thin water film, there exists a typical phenomenon of liquid-liquid slip at the interface between octane and water where the fluid velocity changes rapidly (Zhan et al., 2020a). The apparent viscosity of the liquid at the interface of octane-water is only half of the viscosity of bulk water and octane respectively. The length of the carbon chain also affects the two-phase flow behavior of alkane and water in nanopores of quartz (Xu et al.,

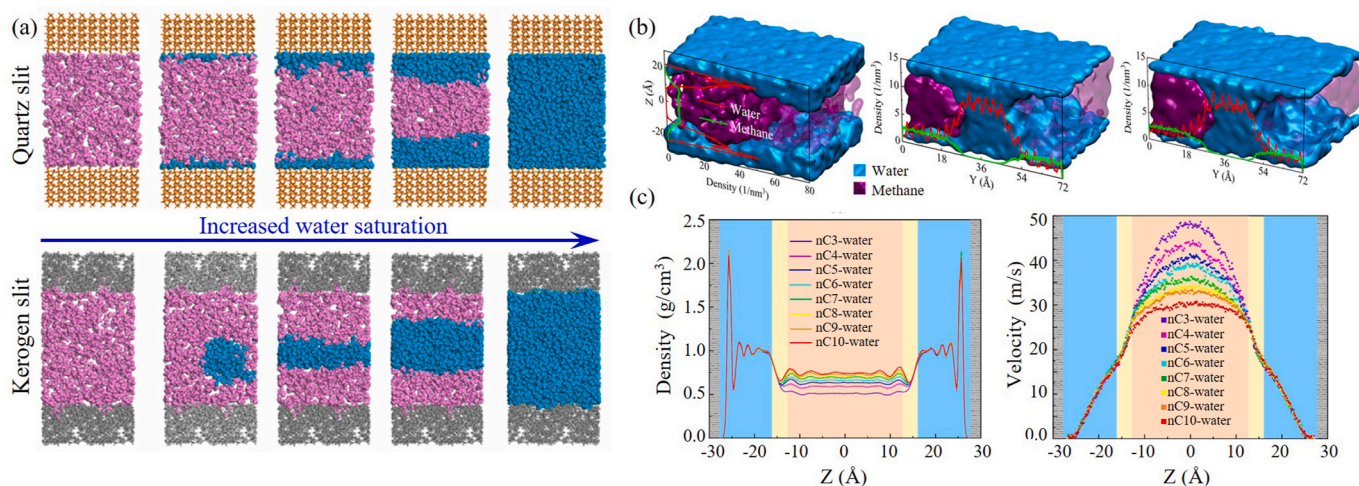


Fig. 6. Fluid molecules and density distribution in nanopores. (a) Water and methane distributions in quartz and kerogen slits for different water saturations (Sang et al., 2022b). (b) Water and methane distributions under different pressures (Liu et al., 2018). (c) Fluid density and velocity profile distribution in different regions of nanopore (Xu et al., 2022).

2022). At the interface region of n-alkane and water, the n-alkane molecules tend to be parallel to the pore surface, and this tendency is accelerated by long n-alkane molecules, resulting in a decrease in the width of the interface region (Fig. 6(c)). In addition, Wang et al. (2024b) found that polar substances such as toluene and asphalt in crude oil would accumulate in the interface area and weaken liquid-liquid slip. These phenomena indicate that the liquid-liquid slip mechanism is complex.

Complex pore structure also influences the transport behavior of fluids in nanoscale pores. He et al. (2015) conducted MD simulations of adsorption and diffusion processes based on randomly generated nanoporous media. The surface area significantly affects the diffusion behavior, and a large surface area corresponds to a small diffusion coefficient. For the description of fluid flow in complex pore topology, MD simulation is limited to a single pore throat structure. Tang et al. (2015) conducted simulations of fluid flow through hourglass-shaped nanopores by varying the cone angle and the length of the cylindrical section.

3.2. CO₂ miscible flow

The CO₂ injection method has been demonstrated to be an effective means of enhanced oil and gas recovery (Lee et al., 2019; Zhou et al., 2019). CO₂ can reduce the interfacial tension and viscosity of crude oil, and induce crude oil swelling and vaporization (Zhang et al., 2018). Under the formation condition, CO₂ is in a supercritical state, and can enter the reservoir to dissolve crude oil (Wu et al., 2016b; Ho and Wang, 2019). As usual, CO₂-enhanced oil recovery (CO₂-EOR) is typically divided into two categories: immiscible and miscible flooding (Cao and Gu, 2013; Jia et al., 2019). Miscible flooding means that CO₂ and oil are miscible, and a mixed phase is formed above the minimum miscible pressure (MMP) (Shokrollahi et al., 2013). Temperature alters the equilibrium between the liquids, which in turn affects the miscible state and MMP in nanopores (Wang et al., 2016b; Sun and Li, 2021). Because the MMP of CO₂ is low and the pressure of the shale reservoir is much greater than the miscible pressure of CO₂ and hydrocarbon, the injected CO₂ is mainly in miscible and near-miscible states (Alharthy et al., 2017; Sambo et al., 2023). Especially in low-permeability oil reservoirs, miscible flooding effectively improves oil recovery (Zhou et al., 2020).

Researchers have studied the diffusion (Mohammed and Mansoori, 2018) and convection (Noorian et al., 2014; Liu et al., 2017) of CO₂ flooding by the MD method. Liu et al. (2017) investigated the micro-mechanism of CO₂ displacing shale oil at different injection rates. They concluded that the miscible zone is primarily comprised of alkane molecules that are isolated from the bulk alkane surface and dissolved in CO₂, and CO₂ molecules that are penetrating into the alkane phase. Yan et al. (2017) studied the transport behavior of oil in nanopores and the influence of CO₂ activating effect (Fig. 7 (a)). CO₂ dissolved in the water phase contributed little to the transport of the oil droplet, while the CO₂ diffused into the oil molecules and weakened the interaction of the oil droplet. As a result, the oil droplets become more stretchable, and the pressure difference needed to overcome the Jamin effect is reduced, facilitating the transport of the oil droplets. Zhou et al. (2020) studied the miscible flow of CO₂ under different velocities and developed a dispersion model considering slip length and boundary conditions. Notably, the convection significantly enhances the miscible process in nanopores, and the enhancement effect is close to the plate velocity. Yuan et al. (2023) explored the adsorption and flow mechanism of CO₂-decane miscible flow in nanoscale pores and quantitatively characterized the changes in CO₂ content in the adsorption layer. They found that CO₂ adsorbed on the surface changes the boundary flow pattern.

Water is present in almost all shale formations, including connate water and water injected by hydraulic fracturing (Wang et al., 2018). Li et al. (2021) explored the distribution mechanism and flow behavior of CO₂ in different water-filled nanopore sizes. Water can be completely displaced by CO₂ in pores with the size of 1 nm. In larger pores, the CO₂ dissolved in the center of the pore space but formed nanoclusters near

the surface (Fig. 7 (b)). According to Henry's law, some CO₂ dissolves in water under pressure, affecting the exposure of oil to CO₂. Dissolved CO₂ reduces the pH of the in-situ water, causing carbonate minerals to dissolve and pore volumes to increase (Sambo et al., 2023). Lee et al. (2019) found that up to 9.5% of CO₂ is stored by the shale matrix due to dissolution, increasing the recovery factor by 2%. In addition, when the oil content is low, a water bridge is formed in the middle of the pore, forming the slug flow (Zhang et al., 2021b). Liu et al. (2022a) found that the injected CO₂ would break through the water bridge, enhancing the flow of the oil and increasing the recovery rate. During the breakthrough process, the adsorbed water film becomes thicker, and the mixing degree of CO₂ and oil increases.

4. Pore scale modeling of multiphase flow and applications

MD simulations fail to obtain the flow behaviors in complex pore systems due to the limited molecule weight, while pore scale simulations become a popular method to explore multiphase flow processes in porous media. Currently, pore scale simulations can address flow behaviors in microporous and nanoporous media by taking into account micro- and nanoscale effects.

4.1. Microscale multiphase flow

Pore scale modeling of multiphase flow can be roughly divided into two categories: pore network model (PNM) and direct numerical simulation (DNS) methods (Liu et al., 2023; Qin et al., 2023). PNM simplifies the complex pore system and can simulate multiphase flow in large-scale models. DNS method retains the actual pore topology and has advantages in describing complex microscopic flow mechanisms.

4.1.1. Numerical simulation method

PNM simplifies the pore structure into a network composed of connected pores and throats, and each pore and throat has specific structural and spatial information. In general, pore structure information can be extracted from the digital core based on the maximum sphere method and central axis method to simplify the pore system and generate PNM (Mehmani et al., 2020). The maximum sphere algorithm was proposed by Silin et al. (2003), but this study did not extract PNM from digital cores. Al-Kharusi and Blunt (2007) applied this method to generate PNM of sandstone and carbonate rocks. Dong (2008) improved the maximum sphere algorithm theory and proposed a clustering algorithm that can clearly divide pores and throats. The central-axis algorithm simplifies the pore space into a topological skeleton and accurately preserves the pore topology. In addition, the established central axis contains redundant branches or multiple central axis nodes. Therefore, after establishing the central axis, redundant branches and unreasonable central axis nodes should be deleted to avoid producing high coordination numbers. In subsequent studies, de Vries et al. (2017) randomly placed spherical micropores with different porosity characteristics into large-scale PNM to construct a two-scale PNM and studied the fluid flow and mass transfer process by adjusting the number of micropore networks and the pore volume fraction. Rabbani et al. (2020) established a three-scale PNM with a large-scale network coupled with fracture and microporous network to simulate gas and liquid flow. Due to the coarse-grained description of the pore geometry, more computational resources are saved in the process of model calculation. It is of great significance for the characterization of multiphase flow on the scale of representative volume elements (Joeekar-Niasar and Hassanizadeh, 2012; Lin et al., 2021; Won et al., 2021). However, due to the homogenization of fluid flow in single pores, the application of this method has significant limitations for the complex displacement process.

The DNS method divides pore systems into multiple computing units to ensure the accuracy of numerical calculations at the pore scale. This feature enables the capture of complex interfacial dynamics. At present, the level set (LS) method, phase field, volume of fluid (VOF) and Lattice

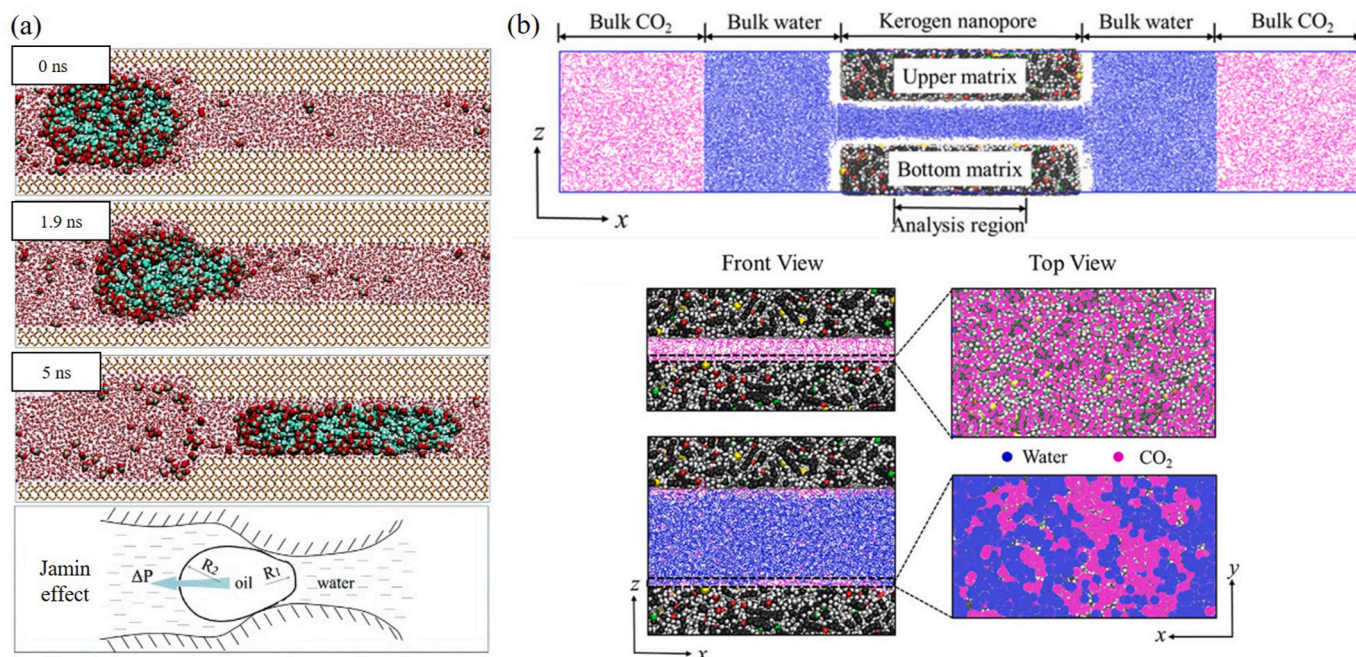


Fig. 7. CO₂ miscible flow in nanopores. Typical snapshots of transport process of oil with CO₂ molecules (Yan et al., 2017). (b) Snapshots of water and CO₂ distribution in different pore sizes (Li et al., 2021).

Boltzmann method (LBM) are widely used pore scale models for simulating displacement behavior. Osher and Sethian (1988) proposed the LS method, which is widely used in fluid dynamics. LS mainly uses the function index defined implicitly by zero contours to determine the immiscible interface position. The function index still follows the evolution of the convection equation in time and space, and combines the discrete interval algorithm to control the immiscible interface (Ning et al., 2023). The VOF method identifies the free surface by analyzing the volume fraction of two-phase fluids in the grid element (Hussain et al., 2023). It is suitable for solving multiphase flow problems with multiple structural interfaces that need to be tracked. The LBM does not capture the dynamic behavior of individual molecules or directly discretize the hydrodynamic equations, but instead focuses on tracking the particle distribution. The fluid is discrete into a large number of virtual particles, and the virtual particles stream and collide on the regular lattice at a certain discrete speed. The governing equation of LBM is the Lattice Boltzmann (LB) equation, which is a discrete equation about the particle distribution function and is completely different from the fluid dynamics equation. However, there is a correlation between the LB equations and the fluid dynamics equations. LB equations can be restored to the Navier-Stokes equations. Therefore, LBM is considered as a second-order precision solution for weakly compressible Navier-Stokes equations.










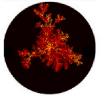




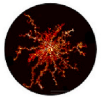












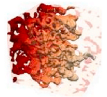





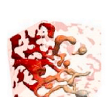
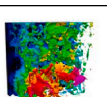
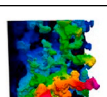
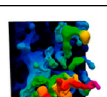
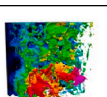
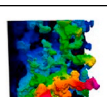
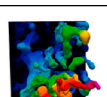
4.1.2. Displacement behavior research

The influence of pore throat structure and connectivity on displacement is significant. Generally, the greater the difference in pore throat size, the worse the connectivity and the more obvious the trapping of non-wetting fluids. A large number of studies on immiscible displacement at the pore scale show that immiscible displacement will exhibit complex flow behavior due to the influence of injection conditions and fluid properties. Table 2 shows the displacement patterns under different capillary numbers and contact angles (Zhao et al., 2016; Bakhshian et al., 2020; Bakhshian et al., 2021; Xiao et al., 2021). Displacement modes can be roughly divided into capillary fingering, viscous fingering, and stable displacement according to the function of capillary number and viscosity ratio (Lenormand et al., 1988). On this basis, Zhang et al. (2011) classified the fluid displacement behavior into

viscous fingering region, capillary fingering region, stable displacement region, and the remaining mixed cross flow patterns through the capillary number and viscosity phase ratio diagram, which directly reflected the influence of the competition between capillary force and viscous force on displacement behavior. In addition, displacement behavior is also affected by pore geometry. Primkulov et al. (2018) studied the mechanism of pore filling processes and showed that the interface merged inside the pore, making the wetting phase fluid adhere to the solid surface. This mechanism depends on the pore geometry and wettability.

Since the displacement front is composed of a large number of curved liquid surfaces, studies have revealed the root cause of the difference in the overall characteristics of the two-phase interface from the movement of curved liquid surfaces in a single pore and the competition and cooperation between liquid surfaces in adjacent pores (Jung et al., 2016). During the drainage, Haines jumps may lead to local imbibition of the wetting phase at the stenosis (Fig. 8(a)), possibly resulting in isolated non-wetting ganglia at the interface front (Al-Gharbi and Blunt, 2005). In the process of drainage, the Haines jump is the main pore scale behavior, in which the influence of inertia force is significant, and the interface variation and the energy dissipation are large (Berg et al., 2013). Under strong wetting conditions, due to the significant capillary effect, interfaces will appear in the pore corner and rough surfaces. These fluid interfaces have priority over the main terminal interface flow under the action of greater capillary pressure. This phenomenon is called corner flow and film flow. Due to the different sources of capillary forces controlling the movement of these interfaces, the corner flow or film flow often exhibits asynchrony with the main terminal interface during imbibition. When the corner flow and film flow pass through the throat, the wetting fluid accumulates and expands, which makes it easy to snap in the throat. Snap-off, as shown in Fig. 8 (b), is more likely to occur in the pore structures with a large pore throat ratio under strong wetting conditions (Singh et al., 2017). The unstable behavior at the interface is not a local phenomenon but depends on the spatial distribution of the previous fluid morphology on the time characteristic scale and exceeds the single pore on the spatial characteristic scale. These small disturbances will accumulate and amplify, resulting in large changes in fluid displacement morphology (Ferrari et al., 2015; Pak

Table 2
Displacing behavior under different conditions.

References	M	$\log_{10}Ca$	Contact angle				
			0-50°	50-70°	70-110°	110-130°	130-180°
Xiao et al. (2021)	0.03	-3.3				/	/
		-4.0				/	/
		-4.6				/	/
Zhao et al. (2016)	0.003	-0.54					
		-1.54					
		-2.54					
Bakhshian et al. (2021)	20	-5.0					
	0.05						
	1			/		/	
Bakhshian et al. (2020)	1	-6.0		/		/	

et al., 2015). In addition, the effects of wettability and pore structure on multiphase flow in complex pore networks can be reflected by variations of macroscopic parameters such as capillary pressure, relative permeability, and inlet pressure. Therefore, by quantifying the microscale flow effect of immiscible displacement, the influence mechanism at the pore scale can be reflected in the macroscopic fluid flow behavior. For the miscible multiphase flow, such as the CO₂-oil-water system, the CO₂ phase not only changes the pore filling mechanism and displacement behavior (Chang et al., 2017) but also changes the macroscopic properties such as effective viscosity (Li et al., 2019; Zhang et al., 2021c), relative permeability and fluid distribution (Yong et al., 2021) through diffusion (Wu et al., 2022), competitive adsorption (Fang et al., 2017) and convection.

4.2. Nanoscale multiphase flow

Pore scale simulations considering capillary effects have been widely used for microscale multiphase flow in complex porous media. While nanoscale multiphase flow involves complex flow mechanisms, including boundary slip, adsorption, and diffusion (Feng et al., 2022), these have not been fully studied in porous media. MD simulations are

used to investigate nanoconfined multiphase flow, which accurately captures various fluid-fluid and fluid-solid interactions. However, this method is computationally expensive and limited to single nanoscale pores, which limits its application in nanoporous media. To this end, considering nanoscale mechanisms in pore scale simulation can obtain satisfactory research results.

4.2.1. Modeling of multiphase flow in nanoporous media

Currently, only a few studies have focused on exploring multiphase flow in nanoconfined pores using pore scale simulations. PNM and DNS methods have been adopted for nanoconfined multiphase flows. The simulations of water-gas and water-oil flow in complex porous media are realized by introducing nanoscale effects in traditional two-phase flow based on PNM (Song et al., 2023). Typically, the initial PNM is saturated with water and non-wetting fluid invades the PNM. Fig. 9 (a) displays the gas-water distribution in equivalent rectangular and triangle water-wet pores after drainage. Fluids are stratified along the pore surface as adsorbed water, bulk water, gas-water interface, and bulk gas. Such stratified fluids correspond to non-uniform flows due to the heterogeneous distribution of viscosity and density, resulting in liquid-liquid slip. However, the velocity of the two phases is continuous

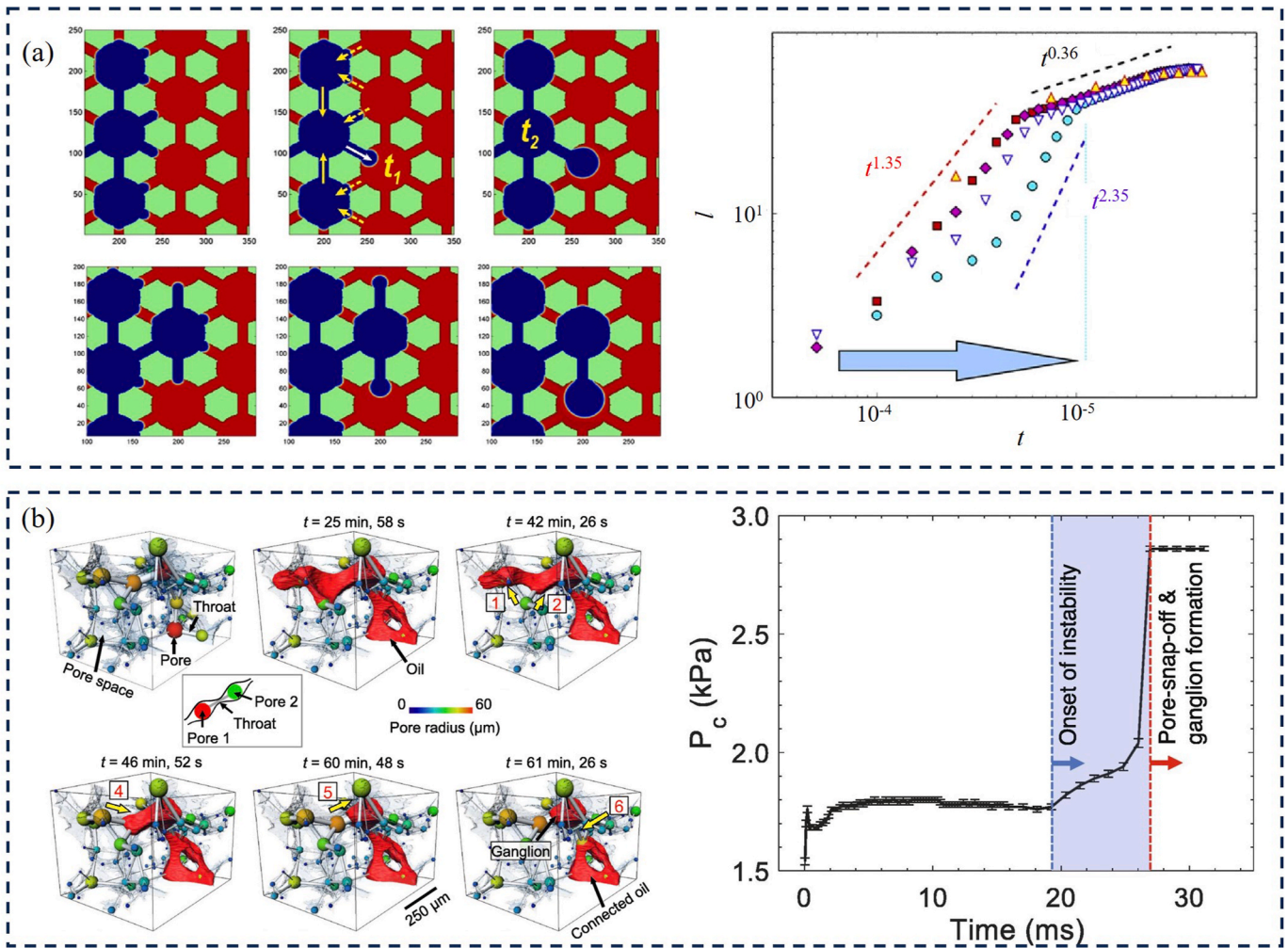


Fig. 8. Pore filling events. (a) Haines jumps during drainage and the interface movement distance versus time (Zacharoudiou and Boek, 2016). (b) Snap off during imbibition and the corresponding change of capillary pressure (Singh et al., 2022).

at the fluid-fluid interface of micropores according to Navier-Stokes equation, which may not be valid in the nanoporous media. There are two types of slip boundary conditions in the pore spaces. One is liquid-solid slip, which represents the slip between the fluid and the solid surface. It is controlled by wettability, and the slip length related to the contact angle varies significantly for different fluids in confined multiphase flows. The other is liquid-liquid slip, which occurs at the fluids interface and is caused by differences in fluids viscosity and density. The interface liquid-liquid slip occurred at the interface region can be divided into no slip, partial slip, and free slip (Feng et al., 2022). Specifically, no slip means that there is no loss of momentum transfer between two phase interfaces; partial slip represents the partial loss of momentum transfer, and free slip means that there is no momentum transfer between the fluid-fluid interface. Kucala et al. (2017) present a fluid dynamics model considering two-phase fluid interfacial slip, to characterize the surface roughness on interfacial slip flow during displacement. They conclude that apparent slip occurs between the invading fluid and the residual fluid trapped in the pits of a rough pore surface and affects the permeability.

In contrast, DNS methods directly solve the multiphase flow process in complex porous media by considering the nanoscale effect. Commonly used slip models for fluid-solid interactions include Navier slip model and Maxwell slip model. Liquid-liquid slip can be solved directly based on the apparent viscosity and density of the stratified regions. Although the pore scale DNS methods considering liquid-liquid slip are computationally intensive, they can capture complex two-phase

flows, such as slug, entrainment, and bubble flow. Zhang et al. (2021a) proposed a pseudo-potential-based LBM to simulate gas-water flow considering fluid-fluid and fluid-solid interactions (Fig. 9 (b)). The model was calibrated by simulating phase separation, Laplacian bubbles, contact angles, and static nanoconfined bubbles, and the simulation results agree with the separation pressure theory.

4.2.2. Influencing factors of nanoscale multiphase flow

Confined multiphase flow in nanoporous media is closely related to the development of unconventional hydrocarbon resources, fuel cells, and geological storage of carbon dioxide. Typically, the pore structure properties of nanoporous materials are complex. Conventional experimental methods are difficult to obtain satisfactory results for nanoconfined multiphase flow and the cost is expensive. However, pore scale simulation may achieve satisfactory results by considering the nanoscale effect, which intuitively captures the residual fluid distribution, relative permeability, and capillary pressure curves of nanoporous media.

Wettability is a key factor affecting nanoconfined multiphase flow, which controls the fluid-solid interaction and near-wall viscosity. Ma et al. (2014) obtained the hydrophobic nanoporous structure of fuel cells based on focused ion beam scanning electron microscopy and improved the PNM considering slip flow and Knudsen diffusion. They conclude that the inlet pressure increases with increasing contact angle. The variation of capillary pressure curves at different contact angles under strong hydrophobic conditions are basically consistent, corresponding to similar pore filling processes. In addition, understanding the relative

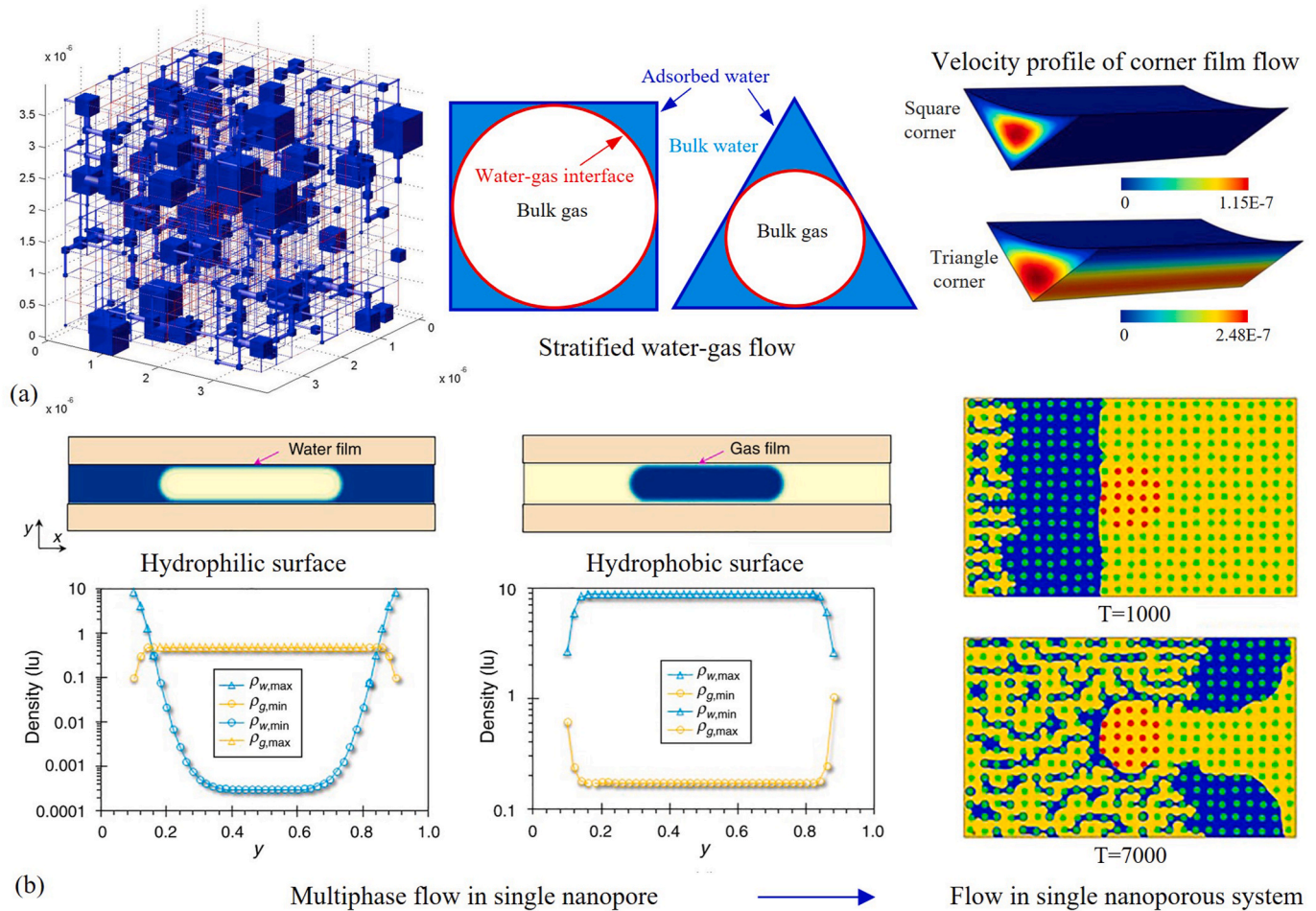


Fig. 9. Pore scale modeling methods for multiphase flow in nanoporous media. (a) PNM (Cui et al., 2019); (b) DNS method (Zhang et al., 2021a).

permeability and residual fluid distribution of nanoporous materials helps the efficient development of unconventional hydrocarbon resources. A large number of nanopores are distributed in both organic and inorganic matter in unconventional reservoirs, which show different wettability and flow characteristics. Song et al. (2018) constructed a 3D hydrophobic PNM based on 2D scanning electron microscope images of shale to simulate the water flooding process considering the nanoscale effects such as adsorption, surface diffusion, and slip (Fig. 10 (a)). They concluded that small pore size leads to increased gas relative permeability and decreased water relative permeability due to the gas adsorption layer on the surface. Cui et al. (2019) constructed a PNM that can properly distinguish organic and inorganic pores based on the actual shale pore size distribution curves; the water-oil flow simulations were carried out by establishing the slip length and corner flow models of circular, square, and equilateral triangular pores. They concluded that the slip effect has a significant influence on relative permeability curves. Zhang et al. (2022b) carried out the water flooding simulation based on mixed wetting PNM considering adsorption and slip effect; the water relative permeability increases and the oil flow capacity decreases slightly compared with no slip condition; the increase in total organic carbon (TOC) content leads to a narrowing of the oil-water coexistence zone of the relative permeability curves and a significant increase in the residual oil saturation.

As for DNS methods, it can capture complex flow patterns, so it has a more accurate description of pore filling mechanisms and residual fluid distribution. Zhang et al. (2021a) simulated gas-water flow in dual-wettability nanoporous media using pseudo-potential LBM. They concluded that isolated organic matter impedes the flow of water,

resulting in high residual gas saturation. Wang et al. (2022) proposed a nanoscale multi-relaxation-time multicomponent and multiphase LBM to investigate water-oil flow considering liquid-solid slip, liquid-liquid slip, and heterogeneous viscosity. They concluded that liquid-solid slip can increase oil-water flow capacity but decrease relative permeability; the liquid-liquid interface slip can increase the relative permeability of the non-wetting phase; the higher the TOC content, the lower the oil relative permeability (Fig. 10 (b)). In addition, Wang et al. (2023b) further developed multicomponent and multiphase LBM for oil- CO_2 competitive adsorption and the oil- CO_2 miscible flow. They discussed the effect of CO_2 -oil miscibility on water-oil flow (Fig. 10 (c)).

5. Reservoir simulation considering micro- and nanoscale effects

Underground reservoirs are huge porous media systems (Okoroafor et al., 2022), and a large number of primary and secondary pores will be formed due to sedimentation, dissolution, etc. (Nolansnyder and Parnell, 2019). These pores are interconnected to form storage spaces. It is known that the reservoir matrix contains formation water and hydrocarbon resources, which leads to multiphase flow in multiscale structures (Yang et al., 2019; Yu et al., 2021). Understanding the multiphase flow mechanism in reservoirs is crucial for the effective exploration and development of hydrocarbon resources. For the simulation of large-scale underground multiphase flow, multiscale effects are obvious for unconventional reservoirs, not only containing a large number of nanoscale pores but also widely developing fractures (Hu et al., 2017, 2022). Hydraulic transition phenomena are significant in multiscale pore

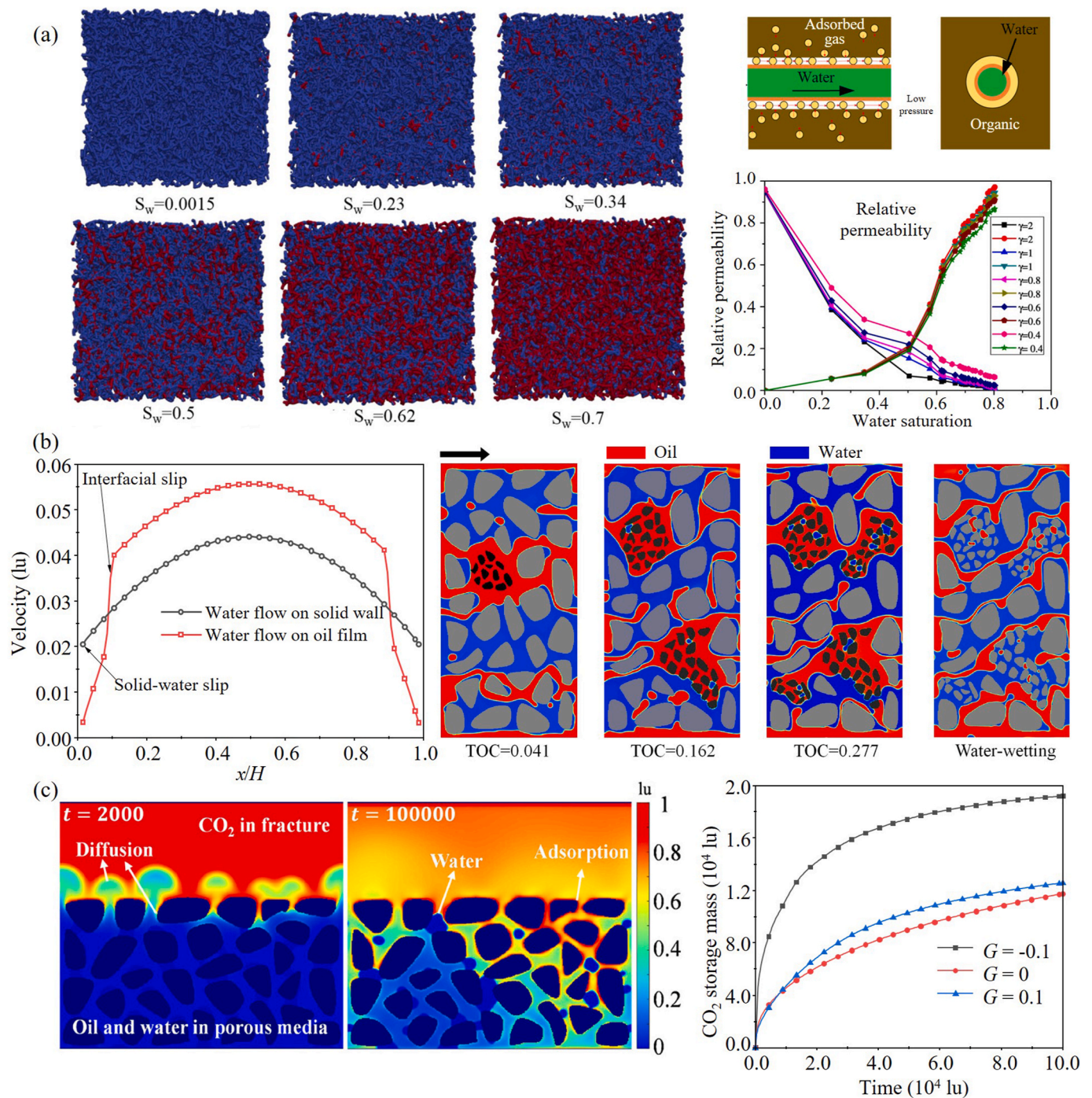


Fig. 10. Pore scale simulation of multiphase and multicomponent flow in nanopores. (a) Nanoscale gas-water flow in hydrophobic PNM of organic pores (Song et al., 2018); (b) Water-oil flow in nanoscale pores considering solid-liquid and liquid-liquid slip (red for oil, blue for water) (Wang et al., 2022); (c) Water-oil- CO_2 multiphase and multicomponent flow in nanopores (Wang et al., 2023b).

structures (Sivanesapillai et al., 2014). Slip flow is significant in nanoscale pores, and as pore size increases, no-slip laminar flow is dominant in microscale pores, while high-speed nonlinear flow may occur in fracture structures. The multiphase flow mechanisms in microporous and nanoporous media are described above by MD and pore scale simulations. However, there are differences in simulation methods and control equations for microscale and macroscale multiphase flow. The equivalent method or homogenization theory is commonly used to establish the multiscale flow model (Fan et al., 2019). In addition, digital cores can be reconstructed based on multiscale images fused with discrete fractures (Huang et al., 2022). The finite element method could

be used for the coupling solution of a multiscale flow process. Therefore, it is necessary to establish a macroscopic multiphase flow model considering micro- and nanoscale effects, and accurately predict the development process of unconventional reservoirs.

The microscopic flow mechanism is complex due to adsorption, dissolution, and diffusion, which makes conventional Darcy's law unusable. The interaction forces between liquid phase molecules and matrix skeleton also need to be considered by introducing slip boundary conditions (Wang et al., 2016a). In addition, widely developed natural and fractured fractures are important storage spaces and migration pathways. Fractal discrete fractures and embedded discrete fractures are

used for the coupling multiscale simulation considering the capillary pressure of micropores and the high conductivity of fractures (Ma et al., 2020). Based on the actual geological data, underground fracture networks can be constructed for simulation (Yang et al., 2022). Meanwhile, with the development of imaging technology, fracture networks can be constructed based on digital cores (He et al., 2023).

Reservoir simulation outputs the fluid pressure and saturation over time. For unconventional reservoirs, fluids flow in multiscale systems, ranging from micro/nanoscale pores to hydraulic fractures up to hundreds of meters in size. This means that conventional reservoir models have difficulty characterizing complex flow behavior in reservoirs. The basic idea of multiscale methods is to integrate fine scale equations into coarse scale equations to solve local flow problems (Abdullah et al., 2019). Zhang et al. (2019b) established a simulation model considering the nanoscale effects and deformation (Fig. 11(a) and (b)). They analyzed the fluid properties in nanopores and predicted the production capacity of the reservoirs. Ran et al. (2023) considered micro- and nanoscale effects (capillary forces and slip flow) in reservoir simulation and derived an apparent permeability model with slip boundary conditions. They found that the production rate was 6% lower than that not considering micro- and nanoscale effects. In addition, Xiao et al. (2023) proposed an apparent permeability model for shale gas reservoirs and incorporated the apparent permeability models into reservoir simulation (Fig. 11(c) and (d)). The influence of micro- and nanoscale effects

on gas production was studied. They found that ignoring the micro- and nanoscale effects have a significant impact on gas production. The difference in cumulative gas production between considering and not considering micro- and nanoscale effects is 19.5%. Therefore, considering micro- and nanoscale flow mechanisms in macroscopic models can make simulation results more accurate.

6. Conclusions and outlook

Multiphase flow is a common scenario in industrial processes. Conventional continuous-scale homogeneous models have been extensively explored. However, the micro- and nanoscale multiphase flow processes are complex due to adsorption, diffusion, slip, and capillary effects. Since underground reservoirs contain a large number of micro- and nanoscale pores, fluid-fluid and fluid-solid interaction mechanisms may significantly affect macroscopic flow performance at the reservoir scale. This review systematically investigates the mechanisms of micro- and nanoscale flow, including the capillary and slip effects involved in immiscible flows, and the diffusion and convection effects required for miscible flows. MD simulations are introduced to explain multiphase flow mechanisms in single nanopores from atomic and molecular perspectives. Based on this, the pore scale simulation methods are developed for simulating complex flow behaviors in nanoporous and microporous media. To highlight the practical implications of micro-

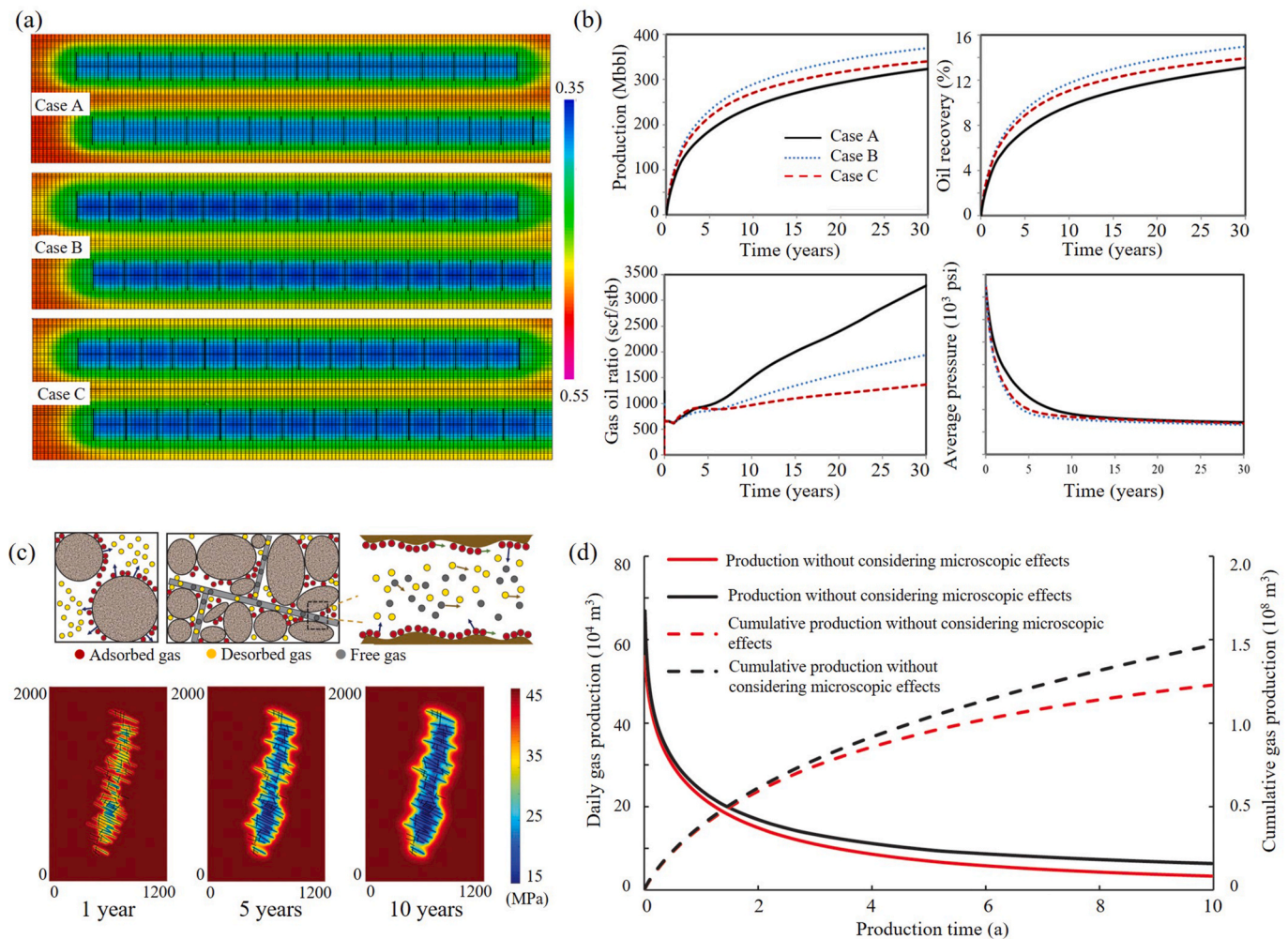


Fig. 11. Reservoir scale simulation considering micro- and nanoscale effects. (a) Oil saturation after production in three cases: case A (without confinement effect), case B (with confinement effect), and case C (with confinement effect and stress-dependent deformation). (b) Oil production process under three conditions (Zhang et al., 2019b). (c) Pressure distribution of shale gas fracturing wells. (d) Shale gas production with and without considering micro- and nanoscale effects (Xiao et al., 2023).

and nanoscale effects, the impact of micro- and nanoscale effects on reservoir scale multiphase flows is analyzed for guiding production. It is worth noting that this review focuses on applications of multiphase flow modeling, while the specific numerical simulation algorithms are not discussed in depth.

Furthermore, the review systematically describes micro- and nanoscale multiphase flow mechanisms that are difficult to characterize experimentally. This has practical significance for an in-depth understanding of the development of unconventional hydrocarbon resources and the microscopic mechanism of carbon dioxide geological sequestration. The underground reservoirs contain a large proportion of micro- and nanoscale pores. MD and pore scale simulations help understand the flow characteristics inside the reservoirs. Specifically, MD simulations obtain the adsorption, diffusion, capillary, and slip effects in single nanopores; the complex displacement process in porous systems can be explained based on the developed pore scale simulations. Existing studies have shown that exploring micro- and nanoscale flows is of practical significance. The difference in production between considering and not considering micro- and nanoscale effects is close to 20% (Xiao et al., 2023). In fact, this effect is related to the pore structure properties of reservoirs and is significant in tight reservoirs. Therefore, accounting for slip and capillary effects in macroscale multiphase flow simulations can help accurately predict production processes. Development processes can be optimized according to the micro- and nanoscale simulation results.

For future research directions, MD simulation methods can be combined with pore scale simulation methods to improve the modeling scale. Unconventional reservoirs face extreme in-situ conditions, and fluid flow properties, wettability, heat and mass transfer parameters are difficult to characterize experimentally. MD simulations can calculate these parameters, correct the pore scale simulation parameters, and thus accurately predict the complex flow process in nanoporous media. Although pore scale simulations provide insights into displacement patterns, fluid distribution, relative permeability, etc., they are computationally expensive. Applying the developing deep learning algorithms to predict complex flow processes can accelerate computation. The existing PoreFlow-Net (Santos et al., 2020) and physical-informed Unet network (Zhao et al., 2024) have been proposed for the prediction of flow fields in microporous media. More convolutional neural network algorithms need to be explored to predict dynamic displacement processes and residual flow distributions in multiphase flows. In addition, the multiphase transport mechanisms involving CO₂ are complex under in situ reservoir conditions. Supercritical CO₂ dissolves in water and oil by convection and diffusion. This causes the aqueous solution to become acidic and react chemically with the rock, affecting the flow process. Thus, attention should be paid to multiphase multi-component flows that consider miscibility, diffusion, and reaction for enhanced hydrocarbon recovery and CO₂ storage efficiency. For reservoir simulations, the pore structures are usually assumed to be homogeneous, which does not conform to the actual characteristics of unconventional reservoirs. Therefore, reservoir simulation methods coupling of heterogeneous pore-fracture structures should be further developed to comprehensively reflect the influence of micro- and nanoscale effects on macroscopic multiphase flows.

CRedit authorship contribution statement

Jianchao Cai: Methodology, Investigation, Conceptualization. **Xiangjie Qin:** Writing – review & editing, Writing – original draft, Investigation. **Xuanzhe Xia:** Writing – review & editing, Methodology, Investigation. **Xinghe Jiao:** Writing – review & editing, Supervision, Investigation. **Hao Chen:** Writing – review & editing, Supervision, Investigation. **Han Wang:** Supervision, Investigation, Formal analysis. **Yuxuan Xia:** Supervision, Methodology, Investigation.

Declaration of competing interest

The authors declare that they have no known competing financial interests or personal relationships that could have appeared to influence the work reported in this paper.

Data availability

No data was used for the research described in the article.

Acknowledgments

This work was supported by National Natural Science Foundation of China (Nos. 42172159, 42302143), China Postdoctoral Science Foundation (No. 2023M743870), and Postdoctoral Fellowship Program of CPSF (No. GZB20230864).

References

- Abdullah, M.A., Panda, A., Gupta, S., Joshi, S., Singh, A., Rao, N., 2019. Multi-scale method for modeling and simulation of two phase flow in reservoir using MDST. *Petrol. Coal* 61 (3), 546–558.
- Ahmadi, M., Aliabadian, E., Liu, B., Lei, X., Khalilpoorkordi, P., Hou, Q., et al., 2022. Comprehensive review of the interfacial behavior of water/oil/surfactant systems using dissipative particle dynamics simulation. *Adv. Colloid Interface Sci.* 309, 102774.
- Al-Gharbi, M.S., Blunt, M.J., 2005. Dynamic network modeling of two-phase drainage in porous media. *Phys. Rev. E* 71, 016308.
- Al-Kharusi, A.S., Blunt, M.J., 2007. Network extraction from sandstone and carbonate pore space images. *J. Petrol. Sci. Eng.* 56 (4), 219–231.
- Alharthy, N., Teklu, T., Kazemi, H., Graves, R., Hawthorne, S., Braunberger, J., et al., 2017. Enhanced oil recovery in liquid-rich shale reservoirs: laboratory to field. *SPE Reservoir Eval. Eng.* 21 (1), 137–159.
- Baban, A., Keshavarz, A., Amin, R., Iglaue, S., 2023. Residual trapping of CO₂ and enhanced oil recovery in oil-wet sandstone core-A three-phase pore-scale analysis using NMR. *Fuel* 332, 126000.
- Bakhshian, S., Hosseini, S.A., Shokri, N., 2019. Pore-scale characteristics of multiphase flow in heterogeneous porous media using the lattice Boltzmann method. *Sci. Rep.* 9 (1), 3377.
- Bakhshian, S., Rabbani, H.S., Hosseini, S.A., Shokri, N., 2020. New insights into complex interactions between heterogeneity and wettability influencing two-phase flow in porous media. *Geophys. Res. Lett.* 47 (14), e2020GL088187.
- Bakhshian, S., Rabbani, H.S., Shokri, N., 2021. Physics-driven investigation of wettability effects on two-phase flow in natural porous media: recent advances, new insights, and future perspectives. *Transp. Porous Media* 140 (1), 85–106.
- Berg, S., Ott, H., Klapp, S.A., Schwing, A., Neiteler, R., Brussee, N., et al., 2013. Real-time 3D imaging of Haines jumps in porous media flow. *Proc. Natl. Acad. Sci. USA* 110 (10), 3755–3759.
- Bitsanis, I., Magda, J.J., Tirrell, M., Davis, H.T., 1987. Molecular dynamics of flow in micropores. *J. Chem. Phys.* 87 (3), 1733–1750.
- Bitsanis, I., Vanderlick, T.K., Tirrell, M., Davis, H.T., 1988. A tractable molecular theory of flow in strongly inhomogeneous fluids. *J. Chem. Phys.* 89 (5), 3152–3162.
- Bui, T., Phan, A., Cole, D.R., Striolo, A., 2017. Transport mechanism of guest methane in water-filled nanopores. *J. Phys. Chem. C* 121 (29), 15675–15686.
- Cai, J., Jiao, X., Wang, H., He, W., Xia, Y., 2024a. Multiphase fluid-rock interactions and flow behaviors in shale nanopores: A comprehensive review. *Earth-Sci. Rev.* 257, 104884.
- Cai, J., Lin, D., Singh, H., Zhou, S., Meng, Q., Zhang, Q., 2019. A simple permeability model for shale gas and key insights on relative importance of various transport mechanisms. *Fuel* 252, 210–219.
- Cai, J., Perfect, E., Cheng, C.-L., Hu, X., 2014. Generalized modeling of spontaneous imbibition based on Hagen-Poiseuille flow in tortuous capillaries with variably shaped apertures. *Langmuir* 30 (18), 5142–5151.
- Cai, J., Qin, X., Wang, H., Xia, Y., Zou, S., 2024. Pore-scale investigation of forced imbibition in porous rocks through interface curvature and pore topology analysis. *J. Rock Mech. Geotech. Eng.* <https://doi.org/10.1016/j.jrmge.2024.02.047>.
- Cao, M., Gu, Y., 2013. Oil recovery mechanisms and asphaltene precipitation phenomenon in immiscible and miscible CO₂ flooding processes. *Fuel* 109, 157–166.
- Chalmers, G.R., Bustin, R.M., Power, I.M., 2012. Characterization of gas shale pore systems by porosimetry, pycnometry, surface area, and field emission scanning electron microscopy/transmission electron microscopy image analyses: examples from the Barnett, Woodford, Haynesville, Marcellus, and Doig units. *AAPG Bull.* 96 (6), 1099–1119.
- Chang, C., Zhou, Q., Oostrom, M., Kneafsey, T.J., Mehta, H., 2017. Pore-scale supercritical CO₂ dissolution and mass transfer under drainage conditions. *Adv. Water Resour.* 100, 14–25.
- Chen, L., He, A., Zhao, J., Kang, Q., Li, Z.-Y., Carmeliet, J., et al., 2022. Pore-scale modeling of complex transport phenomena in porous media. *Prog. Energy Combust. Sci.* 88, 100968.

- Chen, L., Wang, S.-Y., Xiang, X., Tao, W.-Q., 2020. Mechanism of surface nanostructure changing wettability: a molecular dynamics simulation. *Comput. Mater. Sci.* 171, 109223.
- Cui, R., Feng, Q., Chen, H., Zhang, W., Wang, S., 2019. Multiscale random pore network modeling of oil-water two-phase slip flow in shale matrix. *J. Petrol. Sci. Eng.* 175, 46–59.
- de Vries, E.T., Raouf, A., van Genuchten, M.T., 2017. Multiscale modelling of dual-porosity porous media; a computational pore-scale study for flow and solute transport. *Adv. Water Resour.* 105, 82–95.
- Dong, H., 2008. Micro-CT Imaging and Pore Network Extraction, Department of Earth Science and Engineering. Imperial College London.
- Dong Sung, K., Kwang-Cheol, L., Tai Hun, K., Seung, S.L., 2002. Micro-channel filling flow considering surface tension effect. *J. Micromech. Microeng.* 12 (3), 236.
- Etmiman, A., Muzychka, Y.S., Pope, K., 2023. Experimental and numerical analysis of heat transfer and flow phenomena in Taylor flow through a straight mini-channel. *ASME J. Heat Mass Tran.* 145 (8), 081801.
- Fan, W.P., Sun, H., Yao, J., Fan, D.Y., Yang, Y.F., 2019. Homogenization approach for liquid flow within shale system considering slip effect. *J. Clean. Prod.* 235, 146–157.
- Fang, T., Wang, M., Wang, C., Liu, B., Shen, Y., Dai, C., et al., 2017. Oil detachment mechanism in CO₂ flooding from silica surface: molecular dynamics simulation. *Chem. Eng. Sci.* 164, 17–22.
- Fard, M.G., Stiriba, Y., Gaurich, B., Vial, C., Grau, F.X., 2020. Euler-Euler large eddy simulations of the gas-liquid flow in a cylindrical bubble column. *Nucl. Eng. Des.* 369, 110823.
- Farnoud, A., Tofghian, H., Baumann, I., Garcia, G.J.M., Schmid, O., Gutheil, E., et al., 2020. Large eddy simulations of airflow and particle deposition in pulsating bi-directional nasal drug delivery. *Phys. Fluids* 32 (10), 101905.
- Feng, D., Chen, Z., Wu, K., Li, J., Dong, X., Peng, Y., et al., 2022. A comprehensive review on the flow behaviour in shale gas reservoirs: multi-scale, multi-phase, and multi-physics. *Can. J. Chem. Eng.* 100 (11), 3084–3122.
- Feng, Y., Hou, J., Yang, Y., Wang, S., Wang, D., Cheng, T., You, Z., 2022. Morphology of MoS₂ nanosheets and its influence on water/oil interfacial tension: a molecular dynamics study. *Fuel* 312, 122938.
- Ferrari, A., Jimenez-Martinez, J., Borgne, T.L., Méheust, Y., Lunati, I., 2015. Challenges in modeling unstable two-phase flow experiments in porous micromodels. *Water Resour. Res.* 51 (3), 1381–1400.
- Foroozesh, J., Kumar, S., 2020. Nanoparticles behaviors in porous media: application to enhanced oil recovery. *J. Mol. Liq.* 316, 113876.
- Gilron, J., Soffer, A., 2002. Knudsen diffusion in microporous carbon membranes with molecular sieving character. *J. Membr. Sci.* 209 (2), 339–352.
- Gogoi, S., Gogoi, S.B., 2019. Review on microfluidic studies for EOR application. *J. Pet. Explor. Prod. Technol.* 9, 2263–2277.
- Golparvar, A., Zhou, Y., Wu, K., Ma, J., Yu, Z., 2018. A comprehensive review of pore scale modeling methodologies for multiphase flow in porous media. *Adv. Geo-Energy Res.* 2 (4), 418–440.
- Gong, L., Shi, J., Ding, B., Huang, Z.-Q., Sun, S.-Y., Yao, J., 2020. Molecular insight on competitive adsorption and diffusion characteristics of shale gas in water-bearing channels. *Fuel* 278, 118406.
- He, L., Gui, F., Hu, M., Li, D., Zha, W., Tan, J., 2023. Digital core image reconstruction based on residual self-attention generative adversarial networks. *Comput. Geosci.* 27 (3), 499–514.
- He, S., Jiang, Y., Conrad, J.C., Qin, G., 2015. Molecular simulation of natural gas transport and storage in shale rocks with heterogeneous nano-pore structures. *J. Petrol. Sci. Eng.* 133, 401–409.
- He, Y., Cheng, J., Dou, X., Wang, X., 2017. Research on shale gas transportation and apparent permeability in nanopores. *J. Nat. Gas Sci. Eng.* 38, 450–457.
- Ho, T.A., Wang, Y., 2019. Enhancement of oil flow in shale nanopores by manipulating friction and viscosity. *Phys. Chem. Chem. Phys.* 21 (24), 12777–12786.
- Hovorka, S.D., Choi, J.-W., Meckel, T.A., Trevino, R.H., Zeng, H., Kordi, M., et al., 2009. Comparing carbon sequestration in an oil reservoir to sequestration in a brine formation—field study. *Energy Proc.* 1 (1), 2051–2056.
- Hu, D.F., Wei, Z.H., Liu, R.B., Wei, X.F., Chen, F.R., Liu, Z.J., 2022. Enrichment control factors and exploration potential of lacustrine shale oil and gas: a case study of Jurassic in the Fuling area of the Sichuan Basin. *Nat. Gas. Ind. B* 9 (1), 1–8.
- Hu, Y., Liu, Y., Can, C., Kang, Y., Wang, X., Huang, M., et al., 2017. Fracture initiation of an inhomogeneous shale rock under a pressurized supercritical CO₂ jet. *Appl. Sci.* 7, 1093.
- Huang, D.M., Sendner, C., Horinek, D., Netz, R.R., Bocquet, L., 2008. Water slippage versus contact angle: a quasiuniversal relationship. *Phys. Rev. Lett.* 101 (22), 226101.
- Huang, T., Wang, Z., Zeng, Q., Dai, A., 2022. A novel method for multiscale digital core reconstruction based on regional superposition algorithm. *J. Petrol. Sci. Eng.* 212, 110302.
- Hussain, S.T., Regenauer-Lieb, K., Zhuravljov, A., Hussain, F., Rahman, S.S., 2023. Asymptotic hydrodynamic homogenization and thermodynamic bounds for upscaling multiphase flow in porous media. *Adv. Geo-Energy Res.* 9 (1), 38–53.
- Javadpour, F., Singh, H., Rabbani, A., Babaei, M., Enayati, S., 2021. Gas flow models of shale: a review. *Energy Fuels* 35 (4), 2999–3010.
- Jia, B., Tsau, J.-S., Barati, R., 2019. A review of the current progress of CO₂ injection EOR and carbon storage in shale oil reservoirs. *Fuel* 236, 404–427.
- Joekar-Niasar, V., Hassanizadeh, S., 2012. Analysis of fundamentals of two-phase flow in porous media using dynamic pore-network models: a review. *Crit. Rev. Environ. Sci. Technol.* 42 (18), 1895–1976.
- Jung, M., Brinkmann, M., Seemann, R., Hiller, T., Sanchez de La Loma, M., Herminghaus, S., 2016. Wettability controls slow immiscible displacement through local interfacial instabilities. *Phys. Rev. Fluids* 1 (7), 074202.
- Kasiteropoulou, D., Karakasidis, T.E., Liakopoulos, A., 2013. Mesoscopic simulation of fluid flow in periodically grooved microchannels. *Comput. Fluids* 74, 91–101.
- Kone, J.-P., Zhang, X., Yan, Y., Hu, G., Ahmadi, G., 2017. Three-dimensional multiphase flow computational fluid dynamics models for proton exchange membrane fuel cell: a theoretical development. *J. Comput. Multiphase Flows* 9 (1), 3–25.
- Kreutzer, M.T., Kapteijn, F., Moulijn, J.A., Heiszwolf, J.J., 2005. Multiphase monolith reactors: chemical reaction engineering of segmented flow in microchannels. *Chem. Eng. Sci.* 60 (22), 5895–5916.
- Kucala, A., Martinez, M.J., Wang, Y., Noble, D.R., 2017. The influence of interfacial slip on two-phase flow in rough pores. *Water Resour. Res.* 53 (8), 7281–7295.
- Lee, J.H., Jeong, M.S., Lee, K.S., 2019. Incorporation of multi-phase solubility and molecular diffusion in a geochemical evaluation of the CO₂ huff-n-puff process in liquid-rich shale reservoirs. *Fuel* 247, 77–86.
- Lenormand, R., Touboul, E., Zarcone, C., 1988. Numerical models and experiments on immiscible displacements in porous media. *J. Fluid Mech.* 189, 165–187.
- Li, G., Su, Y., Wang, W., Sun, Q., 2022. Mathematical model and application of spontaneous and forced imbibition in shale porous media-considered forced pressure and osmosis. *Energy Fuels* 36 (11), 5723–5736.
- Li, J., Li, X., Wu, K., Chen, Z.J., Wang, K., Zhong, M., et al., 2017. Methane transport through nanoporous shale with sub-irreducible water saturation. In: SPE Europec Featured at 79th EAGE Conference and Exhibition, D031S007R005.
- Li, L., Wang, C., Li, D., Fu, J., Su, Y., Lv, Y., 2019. Experimental investigation of shale oil recovery from Qianjiang core samples by the CO₂ huff-n-puff EOR method. *RSC Adv.* 9 (49), 28857–28869.
- Li, W., Zhang, M., Nan, Y., Pang, W., Jin, Z., 2021. Molecular dynamics study on CO₂ storage in water-filled kerogen nanopores in shale reservoirs: effects of kerogen maturity and pore size. *Langmuir* 37 (1), 542–552.
- Li, X., Bodziony, F., Yin, M., Marschall, H., Berger, R., Butt, H.-J., 2023. Kinetic drop friction. *Nat. Commun.* 14 (1), 4571.
- Lin, D., Hu, L., Bradford, S.A., Zhang, X., Lo, I.M., 2021. Simulation of colloid transport and retention using a pore-network model with roughness and chemical heterogeneity on pore surfaces. *Water Resour. Res.* 57 (2), e2020WR028571.
- Liu, B., Liu, W., Pan, Z., Yu, L., Xie, Z., Lv, G., et al., 2022a. Supercritical CO₂ breaking through a water bridge and enhancing shale oil recovery: a molecular dynamics simulation study. *Energy Fuels* 36 (14), 7558–7568.
- Liu, B., Qi, C., Zhao, X., Teng, G., Zhao, L., Zheng, H., et al., 2018. Nanoscale two-phase flow of methane and water in shale inorganic matrix. *J. Phys. Chem. C* 122 (46), 26671–26679.
- Liu, B., Wang, C., Zhang, J., Xiao, S., Zhang, Z., Shen, Y., et al., 2017. Displacement mechanism of oil in shale inorganic nanopores by supercritical carbon dioxide from molecular dynamics simulations. *Energy Fuels* 31 (1), 738–746.
- Liu, M., Meakin, P., Huang, H., 2007. Dissipative particle dynamics simulation of multiphase fluid flow in microchannels and microchannel networks. *Phys. Fluids* 19 (3), 033302.
- Liu, P., Nie, B., Zhao, Z., Li, J., Yang, H., Qin, C., 2023. Permeability of micro-scale structure in coal: insights from μ -CT image and pore network modelling. *Gas Sci. Eng.* 111, 204931.
- Liu, Y., Berg, S., Ju, Y., Wei, W., Kou, J., Cai, J., 2022b. Systematic investigation of corner flow impact in forced imbibition. *Water Resour. Res.* 58 (10), e2022WR032402.
- Ma, J., Zhang, X., Jiang, Z., Ostadi, H., Jiang, K., Chen, R., 2014. Flow properties of an intact MPL from nano-tomography and pore network modelling. *Fuel* 136, 307–315.
- Ma, T., Xu, H., Guo, C., Fu, X., Liu, W., Yang, R., 2020. A discrete fracture modeling approach for analysis of coalbed methane and water flow in a fractured coal reservoir. *Geofluids* 2020, 8845348.
- Mehmani, A., Verma, R., Prodanović, M., 2020. Pore-scale modeling of carbonates. *Mar. Petrol. Geol.* 114, 104141.
- Mo, F., Qi, Z., Huang, X., Yan, W., Wang, S., Yuan, Y., et al., 2022. Knudsen diffusion in pore-scale water-bearing shales: modelling and case study. *J. Petrol. Sci. Eng.* 214, 110457.
- Mohammed, S., Mansoori, G.A., 2018. The role of supercritical/dense CO₂ gas in altering aqueous/oil interfacial properties: a molecular dynamics study. *Energy Fuels* 32 (2), 2095–2103.
- Mu, Y., Hu, Z., Guo, Q., Duan, X., Chang, J., Niu, W., et al., 2023. Water distribution in marine shales: based on two-dimensional nuclear magnetic resonance and low-temperature nitrogen adsorption. *Energy Fuels* 37 (7), 5034–5047.
- Ning, H., Qian, S., Zhou, T., 2023. Applications of level set method in computational fluid dynamics: a review. *Int. J. Hydromechatronics* 6 (1), 1–33.
- Nolansnyder, D.R., Parnell, J., 2019. Comparative pore surface area in primary and secondary porosity in sandstones. *J. Petrol. Sci. Eng.* 172, 489–492.
- Noorian, H., Toghaie, D., Azimian, A.R., 2014. Molecular dynamics simulation of Poiseuille flow in a rough nano channel with checker surface roughnesses geometry. *Heat Mass Tran.* 50 (1), 105–113.
- Okoroafor, E.R., Saltzer, S.D., Kovscek, A.R., 2022. Toward underground hydrogen storage in porous media: reservoir engineering insights. *Int. J. Hydrogen Energy* 47 (79), 33781–33802.
- Osher, S., Sethian, J.A., 1988. Fronts propagating with curvature-dependent speed: algorithms based on Hamilton-Jacobi formulations. *J. Comput. Phys.* 79 (1), 12–49.
- Oyarzua, E., Walther, J.H., Mejía, A., Zambrano, H.A., 2015. Early regimes of water capillary flow in slit silica nanochannels. *Phys. Chem. Chem. Phys.* 17 (22), 14731–14739.
- Pak, T., Butler, L.B., Geiger, S., Van Dijke, M.I., Sorbie, K.S., 2015. Droplet fragmentation: 3D imaging of a previously unidentified pore-scale process during multiphase flow in porous media. *Proc. Natl. Acad. Sci. USA* 112 (7), 1947–1952.
- Patel, H., Kuipers, J., Peters, E., 2019. Effect of flow and fluid properties on the mobility of multiphase flows through porous media. *Chem. Eng. Sci.* 193, 243–254.

- Pawar, G., Meakin, P., Huang, H., 2017. Reactive molecular dynamics simulation of kerogen thermal maturation and cross-linking pathways. *Energy Fuels* 31 (11), 11601–11614.
- Primkulov, B.K., Talman, S., Khaleghi, K., Rangriz Shokri, A., Chalaturnyk, R., Zhao, B., et al., 2018. Quasistatic fluid-fluid displacement in porous media: invasion-percolation through a wetting transition. *Phys. Rev. Fluids* 3 (10), 104001.
- Qin, X., Cai, J., Wang, G., 2023. Pore-scale modeling of pore structure properties and wettability effect on permeability of low-rank coal. *Int. J. Min. Sci. Technol.* 33 (5), 573–584.
- Qin, X., Wu, J., Xia, Y., Wang, H., Cai, J., 2024a. Multicomponent image-based modeling of water flow in heterogeneous wet shale nanopores. *Energy* 298, 131367.
- Qin, X., Xia, Y., Qiao, J., Chen, J., Zeng, J., Cai, J., 2024b. Modeling of multiphase flow in low permeability porous media: effect of wettability and pore structure properties. *J. Rock Mech. Geotech. Eng.* 16 (4), 1127–1139.
- Rabbani, A., Babaei, M., Javadpour, F., 2020. A triple pore network model (T-PNM) for gas flow simulation in fractured, micro-porous and meso-porous media. *Transp. Porous Media* 132, 707–740.
- Rahimi-Gorji, M., Debbaud, C., Ghorbaniasl, G., Cosyns, S., Willaert, W., Ceelen, W., 2022. Optimization of intraperitoneal aerosolized drug delivery using computational fluid dynamics (CFD) modeling. *Sci. Rep.* 12 (1), 6305.
- Ran, Q., Zhou, X., Ren, D., Dong, J., Xu, M., Li, R., 2023. Numerical modeling of shale oil considering the influence of micro- and nanoscale pore structures. *Energies* 16 (18), 6482.
- Roy, S., Raju, R., Chuang, H.F., Cruden, B.A., Meyyappan, M., 2003. Modeling gas flow through microchannels and nanopores. *J. Appl. Phys.* 93 (8), 4870–4879.
- Sambo, C., Liu, N., Shaibu, R., Ahmed, A.A., Hashish, R.G., 2023. A technical review of CO₂ for enhanced oil recovery in unconventional oil reservoirs. *Geoenergy Sci. Eng.* 221, 111185.
- Sang, Q., Zhao, X.-Y., Liu, H.-M., Dong, M.-Z., 2022a. Analysis of imbibition of n-alkanes in kerogen slits by molecular dynamics simulation for characterization of shale oil rocks. *Petrol. Sci.* 19 (3), 1236–1249.
- Sang, Q., Zhao, X., Dong, M., 2022b. Effects of water on gas flow in quartz and kerogen nano-slits in shale gas formations. *J. Nat. Gas Sci. Eng.* 107, 104770.
- Santo, K.P., Neimark, A.V., 2021. Dissipative particle dynamics simulations in colloid and interface science: a review. *Adv. Colloid Interface Sci.* 298, 102545.
- Santos, J.E., Xu, D., Jo, H., Landry, C.J., Prodanović, M., Pycrc, M.J., 2020. PoreFlow-Net: a 3D convolutional neural network to predict fluid flow through porous media. *Adv. Water Resour.* 138, 103539.
- Secchi, E., Marbach, S., Niguès, A., Stein, D., Siria, A., Bocquet, L., 2016. Massive radius-dependent flow slippage in carbon nanotubes. *Nature* 537 (7619), 210–213.
- Shokrollahi, A., Arabloo, M., Gharagheizi, F., Mohammadi, A.H., 2013. Intelligent model for prediction of CO₂ – reservoir oil minimum miscibility pressure. *Fuel* 112, 375–384.
- Silin, D.B., Jin, G., Patzek, T.W., 2003. Robust determination of the pore space morphology in sedimentary rocks. In: *SPE Annual Technical Conference and Exhibition: SPE-84296-MS*.
- Singh, K., Bultreys, T., Raeini, A.Q., Shams, M., Blunt, M.J., 2022. New type of pore-snap-off and displacement correlations in imbibition. *J. Colloid Interface Sci.* 609, 384–392.
- Singh, K., Menke, H., Andrew, M., Lin, Q., Rau, C., Blunt, M.J., et al., 2017. Dynamics of snap-off and pore-filling events during two-phase fluid flow in permeable media. *Sci. Rep.* 7 (1), 5192.
- Sivanesapillai, R., Steeb, H., Hartmaier, A., 2014. Transition of effective hydraulic properties from low to high Reynolds number flow in porous media. *Geophys. Res. Lett.* 41 (14), 4920–4928.
- Sofos, F., Karakasis, T.E., Liakopoulos, A., 2010. Effect of wall roughness on shear viscosity and diffusion in nanochannels. *Int. J. Heat Mass Tran.* 53 (19–20), 3839–3846.
- Song, W., Prodanović, M., Yao, J., Zhang, K., 2023. Nano-scale wetting film impact on multiphase transport properties in porous media. *Transp. Porous Media* 149 (1), 5–33.
- Song, W., Yao, J., Ma, J., Sun, H., Li, Y., Yang, Y., et al., 2018. Numerical simulation of multiphase flow in nanoporous organic matter with application to coal and gas shale systems. *Water Resour. Res.* 54 (2), 1077–1092.
- Struchtrup, H., 2005. *Macroscopic Transport Equations for Rarefied Gas Flows, Interaction of Mechanics and Mathematics*. Springer, Heidelberg, Berlin, pp. 145–160.
- Sui, H., Zhang, F., Wang, Z., Wang, D., Wang, Y., 2020. Effect of kerogen maturity, water content for carbon dioxide, methane, and their mixture adsorption and diffusion in kerogen: a computational investigation. *Langmuir* 36 (33), 9756–9769.
- Sun, E.W.-H., Bourg, I.C., 2020. Molecular dynamics simulations of mineral surface wettability by water versus CO₂: thin films, contact angles, and capillary pressure in a silica nanopore. *J. Phys. Chem. C* 124 (46), 25382–25395.
- Sun, H., Li, H., 2021. Minimum miscibility pressure determination in confined nanopores considering pore size distribution of tight/shale formations. *Fuel* 286, 119450.
- Takaba, H., Onumata, Y., Nakao, S.-i., 2007. Molecular simulation of pressure-driven fluid flow in nanoporous membranes. *J. Chem. Phys.* 127 (5), 054703.
- Tang, D., Yoo, Y.-E., Kim, D., 2015. Molecular dynamics simulations on water permeation through hourglass-shaped nanopores with varying pore geometry. *Chem. Phys.* 453–454, 13–19.
- Tang, M., Zhang, T., Ma, Y., Hao, D., Yang, X., Li, Y., 2023. Experimental study on fracture effect on the multiphase flow in ultra-low permeability sandstone based on LF-NMR. *Geoenergy Sci. Eng.* 222, 211399.
- Thomas, J.A., McGaughey, A.J., 2008. Reassessing fast water transport through carbon nanotubes. *Nano Lett.* 8 (9), 2788–2793.
- Tian, W., Wu, K., Chen, Z., Lei, Z., Gao, Y., Li, J., 2022. Mathematical model of dynamic imbibition in nanoporous reservoirs. *Petrol. Explor. Dev.* 49 (1), 170–178.
- Tian, W., Wu, K., Chen, Z., Gao, Y., Li, J., Wang, M., 2022a. A relative permeability model considering nanoconfinement and dynamic contact angle effects for tight reservoirs. *Energy* 258, 124846.
- Tian, Z., Wei, W., Zhou, S., Sun, C., Rezaee, R., Cai, J., 2022b. Impacts of gas properties and transport mechanisms on the permeability of shale at pore and core scale. *Energy* 244, 122707.
- Ufer, A., Mendorf, M., Ghaini, A., Agar, D.W., 2011. Liquid/liquid slug flow capillary microreactor. *Chem. Eng. Technol.* 34 (3), 353–360.
- Ungerer, P., Collell, J., Yiannourakou, M., 2015. Molecular modeling of the volumetric and thermodynamic properties of kerogen: influence of organic type and maturity. *Energy Fuels* 29 (1), 91–105.
- Vandenbroucke, M., Largeau, C., 2007. Kerogen origin, evolution and structure. *Org. Geochem.* 38 (5), 719–833.
- Vega-Sánchez, C., Peppou-Chapman, S., Zhu, L., Neto, C., 2022. Nanobubbles explain the large slip observed on lubricant-infused surfaces. *Nat. Commun.* 13 (1), 351.
- Wang, G., Han, Z., Xu, H., Peng, S., Huang, Q., Long, Q., 2024a. Effect of coal moisture content on gas desorption and diffusion: a theoretical model and numerical solution. *Phys. Fluids* 36 (7), 073109.
- Wang, G., Qin, X., Han, D., Liu, Z., 2021a. Study on seepage and deformation characteristics of coal microstructure by 3D reconstruction of CT images at high temperatures. *Int. J. Min. Sci. Technol.* 31 (2), 175–185.
- Wang, H., Cai, J., Su, Y., Jin, Z., Wang, W., Li, G., 2023a. Imbibition behaviors in shale nanoporous media from pore-scale perspectives. *Capillarity* 9 (2), 32–44.
- Wang, H., Cai, J., Su, Y., Jin, Z., Zhang, M., Wang, W., et al., 2023b. Pore-scale study on shale oil–CO₂–water miscibility, competitive adsorption, and multiphase flow behaviors. *Langmuir* 39 (34), 12226–12234.
- Wang, H., Su, Y., Wang, W., Li, L., Sheng, G., Zhan, S., 2019a. Relative permeability model of oil-water flow in nanoporous media considering multi-mechanisms. *J. Petrol. Sci. Eng.* 183, 106361.
- Wang, H., Wang, W., Su, Y., Jin, Z., 2022. Lattice Boltzmann model for oil/water two-phase flow in nanoporous media considering heterogeneous viscosity, liquid/solid, and liquid/liquid slip. *SPE J.* 27 (6), 3508–3524.
- Wang, S., Feng, Q., Zha, M., Javadpour, F., Hu, Q., 2018. Supercritical methane diffusion in shale nanopores: effects of pressure, mineral types, and moisture content. *Energy Fuels* 32 (1), 169–180.
- Wang, S., Javadpour, F., Feng, Q.H., 2016a. Molecular dynamics simulations of oil transport through inorganic nanopores in shale. *Fuel* 171, 74–86.
- Wang, S., Ma, M., Chen, S., 2016b. Application of PC-SAFT equation of state for CO₂ minimum miscibility pressure prediction in nanopores. In: *SPE Improved Oil Recovery Conference*. Tulsa, Oklahoma, USA.
- Wang, S., Wang, J., Liu, H., Liu, F., 2021b. Impacts of polar molecules of crude oil on spontaneous imbibition in calcite nanoslit: a molecular dynamics simulation study. *Energy Fuels* 35 (17), 13671–13686.
- Wang, W., Xu, J., Zhan, S., Xie, Q., Wang, C., Su, Y., 2024b. Multi-component oil–water two phase flow in quartz and kerogen nanopores: a molecular dynamics study. *Fuel* 362, 130869.
- Won, J., Lee, J., Burns, S.E., 2021. Upscaling polydispersed particle transport in porous media using pore network model. *Acta Geotech.* 16, 421–432.
- Wu, H., Jin, Z., Xu, X., Zhao, S., Liu, H., 2022. Effect of competitive adsorption on the deformation behavior of nanoslit-confined carbon dioxide and methane mixtures. *Chem. Eng. J.* 431, 133963.
- Wu, J., Yang, X., Huang, S., Zhao, S., Zhang, D., Zhang, J., et al., 2023. Molecular simulation of methane adsorption in deep shale nanopores: effect of rock constituents and water. *Minerals* 13 (6), 756.
- Wu, K., Chen, Z., Li, J., Li, X., Xu, J., Dong, X., 2017. Wettability effect on nanoconfined water flow. *Proc. Natl. Acad. Sci. USA* 114 (13), 3358–3363.
- Wu, K., Chen, Z., Li, X., Guo, C., Wei, M., 2016a. A model for multiple transport mechanisms through nanopores of shale gas reservoirs with real gas effect-adsorption-mechanic coupling. *Int. J. Heat Mass Tran.* 93, 408–426.
- Wu, K., Li, X., Wang, C., Yu, W., Chen, Z., 2015. Model for surface diffusion of adsorbed gas in nanopores of shale gas reservoirs. *Ind. Eng. Chem. Res.* 54 (12), 3225–3236.
- Wu, T., Xue, Q., Li, X., Tao, Y., Jin, Y., Ling, C., et al., 2016b. Extraction of kerogen from oil shale with supercritical carbon dioxide: molecular dynamics simulations. *J. Supercrit. Fluids* 107, 499–506.
- Wu, Z., Sun, Z., Shu, K., Jiang, S., Gou, Q., Chen, Z., 2024. Mechanism of shale oil displacement by CO₂ in nanopores: a molecular dynamics simulation study. *Adv. Geo-Energy Res.* 11 (2), 141–151.
- Xiao, H., Zhang, R., Chen, M., Jing, C., Gao, S., Chen, C., et al., 2023. Simulation of the production performances of horizontal wells with a fractured shale gas reservoir. *Fluid Dynam. Mater. Process.* 19 (7), 1803–1815.
- Xiao, L., Zhu, G., Zhang, L., Yao, J., Sun, H., 2021. Effects of pore-size disorder and wettability on forced imbibition in porous media. *J. Petrol. Sci. Eng.* 201, 108485.
- Xiong, H., Devegowda, D., Huang, L., 2020. Water bridges in clay nanopores: mechanisms of formation and impact on hydrocarbon transport. *Langmuir* 36 (3), 723–733.
- Xiong, X., Devegowda, D., Michel Villazon, G.G., Sigal, R.F., Civan, F., 2012. A fully-coupled free and adsorptive phase transport model for shale gas reservoirs including non-Darcy flow effects. *SPE Annual Technical Conference and Exhibition*. Society of Petroleum Engineers, San Antonio, Texas, USA.
- Xu, H., Yu, H., Fan, J., Zhu, Y., Wang, F., Wu, H., 2020. Two-phase transport characteristic of shale gas and water through hydrophilic and hydrophobic nanopores. *Energy Fuels* 34 (4), 4407–4420.

- Xu, J., Zhan, S., Wang, W., Su, Y., Wang, H., 2022. Molecular dynamics simulations of two-phase flow of n-alkanes with water in quartz nanopores. *Chem. Eng. J.* 430, 132800.
- Yan, Y., Dong, Z., Zhang, Y., Wang, P., Fang, T., Zhang, J., 2017. CO₂ activating hydrocarbon transport across nanopore throat: insights from molecular dynamics simulation. *Phys. Chem. Chem. Phys.* 19 (45), 30439–30444.
- Yan, Y., Wang, L., Wang, T., Wang, X., Hu, Y., Duan, Q., 2018. Application of soft computing techniques to multiphase flow measurement: a review. *Flow Meas. Instrum.* 60, 30–43.
- Yang, S., Dehghanpour, H., Binazadeh, M., Dong, P., 2017. A molecular dynamics explanation for fast imbibition of oil in organic tight rocks. *Fuel* 190, 409–419.
- Yang, Y., Liu, F., Yao, J., Iglauer, S., Sajjadi, M., Zhang, K., et al., 2022. In: Multi-scale reconstruction of porous media from low-resolution core images using conditional generative adversarial networks. *J. Nat. Gas Sci. Eng.* 99, 104411.
- Yang, Y., Liu, J., Yao, J., Kou, J., Li, Z., Wu, T., et al., 2020. Adsorption behaviors of shale oil in kerogen slit by molecular simulation. *Chem. Eng. J.* 387, 124054.
- Yang, Y.H., Li, Z., Cui, Z.Q., Sun, H., Lu, X.Q., Yao, J., et al., 2019. Adsorption of coalbed methane in dry and moist coal nanoslits. *J. Phys. Chem. C* 123 (51), 30842–30850.
- Yao, C., Yue, J., Zhao, Y., Chen, G., Yuan, q., 2015. Review on flow and mass transfer characteristics of gas-liquid slug flow in microchannels. *CIESC J.* 66 (8), 2759–2766 (in Chinese).
- Yong, W., Derksen, J., Zhou, Y., 2021. The influence of CO₂ and CH₄ mixture on water wettability in organic rich shale nanopore. *J. Nat. Gas Sci. Eng.* 87, 103746.
- Yong, W., Zhou, Y., 2022. A molecular dynamics investigation on methane flow and water droplets sliding in organic shale pores with nano-structured roughness. *Transp. Porous Media* 144 (1), 69–87.
- Yu, H., Xu, H.Y., Fan, J.C., Zhu, Y.B., Wang, F.C., Wu, H.A., 2021. Transport of shale gas in microporous/nanoporous media: molecular to pore-scale simulations. *Energy Fuels* 35 (2), 911–943.
- Yuan, L., Zhang, Y., Liu, S., Zhang, J., Song, Y., 2023. Molecular dynamics simulation of CO₂-oil miscible fluid distribution and flow within nanopores. *J. Mol. Liq.* 380, 121769.
- Zacharoudiou, I., Boek, E.S., 2016. Capillary filling and Haines jump dynamics using free energy Lattice Boltzmann simulations. *Adv. Water Resour.* 92, 43–56.
- Zhan, S., Su, Y., Jin, Z., Wang, W., Li, L., 2020a. Effect of water film on oil flow in quartz nanopores from molecular perspectives. *Fuel* 262, 116560.
- Zhan, S., Su, Y., Jin, Z., Zhang, M., Wang, W., Hao, Y., et al., 2020b. Study of liquid-liquid two-phase flow in hydrophilic nanochannels by molecular simulations and theoretical modeling. *Chem. Eng. J.* 395, 125053.
- Zhang, C., Oostrom, M., Wietsma, T.W., Grate, J.W., Warner, M.G., 2011. Influence of viscous and capillary forces on immiscible fluid displacement: pore-scale experimental study in a water-wet micromodel demonstrating viscous and capillary fingering. *Energy Fuels* 25 (8), 3493–3505.
- Zhang, H., Ahmed, M., Zhan, J.-H., 2022a. Recent advances in molecular simulation of oil shale kerogen. *Fuel* 316, 123392.
- Zhang, L., Shan, B., Zhao, Y., Guo, Z., 2019a. Review of micro seepage mechanisms in shale gas reservoirs. *Int. J. Heat Mass Tran.* 139, 144–179.
- Zhang, N., Wei, M., Bai, B., 2018. Statistical and analytical review of worldwide CO₂ immiscible field applications. *Fuel* 220, 89–100.
- Zhang, T., Hu, Q., Tian, Q., Ke, Y., Wang, Q., 2024. Small angle neutron scattering studies of shale oil occurrence status at nanopores. *Adv. Geo-Energy Res.* 11 (3), 230–240.
- Zhang, T., Javadpour, F., Li, J., Zhao, Y., Zhang, L., Li, X., 2021a. Pore-scale perspective of gas/water two-phase flow in shale. *SPE J.* 26 (2), 828–846.
- Zhang, T., Li, X., Sun, Z., Feng, D., Miao, Y., Li, P., et al., 2017. An analytical model for relative permeability in water-wet nanoporous media. *Chem. Eng. Sci.* 174, 1–12.
- Zhang, W., Feng, Q., Jin, Z., Xing, X., Wang, S., 2021b. Molecular simulation study of oil-water two-phase fluid transport in shale inorganic nanopores. *Chem. Eng. Sci.* 245, 116948.
- Zhang, W., Feng, Q., Wang, S., Xing, X., Jin, Z., 2021c. CO₂-regulated octane flow in calcite nanopores from molecular perspectives. *Fuel* 286, 119299.
- Zhang, W., Feng, Q., Wang, S., Zhang, J., Jin, Z., Xia, T., et al., 2022b. Pore network modeling of oil and water transport in nanoporous shale with mixed wettability. *J. Petrol. Sci. Eng.* 209, 109884.
- Zhang, Y., Di, Y., Liu, P., Li, W., 2019b. Simulation of tight fluid flow with the consideration of capillarity and stress-change effect. *Sci. Rep.* 9 (1), 5324.
- Zhao, B., MacMinn, C.W., Juanes, R., 2016. Wettability control on multiphase flow in patterned microfluidics. *Proc. Natl. Acad. Sci. USA* 113 (37), 10251–10256.
- Zhao, J., Liu, Y., Qin, F., Fei, L., 2023. Pore-scale fluid flow simulation coupling lattice Boltzmann method and pore network model. *Capillarity* 7 (3), 41–46.
- Zhao, J., Wu, J., Wang, H., Xia, Y., Cai, J., 2024. Single phase flow simulation in porous media by physical-informed Unet network based on lattice Boltzmann method. *J. Hydrol.* 639, 131501.
- Zhou, X., Yuan, Q., Rui, Z., Wang, H., Feng, J., Zhang, L., et al., 2019. Feasibility study of CO₂ huff 'n' puff process to enhance heavy oil recovery via long core experiments. *Appl. Energy* 236, 526–539.
- Zhou, Y., Ai, L., Chen, M., 2020. Taylor dispersion in nanopores during miscible CO₂ flooding: molecular dynamics study. *Ind. Eng. Chem. Res.* 59 (40), 18203–18210.
- Zhu, X., Wang, S., Feng, Q., Zhang, L., Chen, L., Tao, W., 2021. Pore-scale numerical prediction of three-phase relative permeability in porous media using the lattice Boltzmann method. *Int. Commun. Heat Mass Tran.* 126, 105403.